Inorganic Chemistry
Article

*Inorg. Chem.* **2010**, *49*, 8873–8885 **8873**
DOI: 10.1021/ic101041m

# Sulfur Donor Atom Effects on Copper(I)/$O_2$ Chemistry with Thioanisole Containing Tetradentate $N_3S$ Ligand Leading to $\mu$-1,2-Peroxo-Dicopper(II) Species

**Yunho Lee,[†] Dong-Heon Lee,[‡] Ga Young Park,[†] Heather R. Lucas,[†] Amy A. Narducci Sarjeant,[†] Matthew T. Kieber-Emmons,[§] Michael A. Vance,[§] Ashley E. Milligan,[§] Edward I. Solomon,[§] and Kenneth D. Karlin*[,†]**

[†]*Department of Chemistry, the Johns Hopkins University, Baltimore, Maryland 21218,*
[‡]*Department of Chemistry, Chonbuk National University, Jeonju, S. Korea 561-756, and*
[§]*Department of Chemistry, Stanford University, Stanford, California 94305*

Received May 24, 2010

To better understand the effect of thioether coordination in copper-$O_2$ chemistry, the tetradentate $N_3S$ ligand $L^{ASM}$ (2-(methylthio)-*N,N*-bis((pyridin-2-yl)methyl)benzenamine) and related alkylether ligand $L^{EOE}$ (2-ethoxy-*N,N*-bis((pyridin-2-yl)methyl)ethanamine) have been studied. The corresponding copper(I) complexes, $[(L^{ASM})Cu^{I}]^{+}$ (**1a**) and $[(L^{EOE})Cu^{I}]^{+}$ (**3a**), were studied as were the related compound $[(L^{ESE})Cu^{I}]^{+}$ (**2a**, $L^{ESE}$ = (2-ethylthio-*N,N*-bis((pyridin-2-yl)methyl)ethanamine). The X-ray structure of **1a** and its solution conductivity reveal a monomeric molecular structure possessing thioether coordination which persists in solution. In contrast, the C−O stretching frequencies of the derivative Cu(I)-CO complexes reveal that for these complexes, the modulated ligand arms, whether arylthioether, alkylthioether, or ether, are not coordinated to the cuprous ion. Electrochemical data for **1a** and **2a** in $CH_3CN$ and *N,N*-dimethylformamide (DMF) show the thioanisole moiety to be a poor electron donor compared to alkylthioether (**1a** is ∼200 mV more positive than **2a**). The structures of $[(L^{ASM})Cu^{II}(CH_3OH)]^{2+}$ (**1c**) and $[(L^{ESE})Cu^{II}(CH_3OH)]^{2+}$ (**2c**) have also been obtained and indicate nearly identical copper coordination environments. Oxygenation of **1a** at reduced temperature gives a characteristic deep blue intermediate $[\{(L^{ASM})Cu^{II}\}_2(O_2^{2-})]^{2+}$ (**1b$^{P}$**) with absorption features at 442 (1,500 $M^{-1}$ $cm^{-1}$), 530 (8,600 $M^{-1}$ $cm^{-1}$), and 605 nm (10,400 $M^{-1}$ $cm^{-1}$); these values compare well to the ligand-to-metal charge-transfer (LMCT) transitions previously reported for $[\{(L^{ESE})Cu^{II}\}_2(O_2^{2-})]^{2+}$ (**2b$^{P}$**). Resonance Raman data for $[\{(L^{ASM})Cu^{II}\}_2(O_2^{2-})]^{2+}$ (**1b$^{P}$**) support the formation of $\mu$-1,2-peroxo species $\nu$(O−O) = 828 $cm^{-1}$($\Delta(^{18}O_2)$ = 48), $\nu_{sym}$(Cu−O) = 547 $cm^{-1}$ ($\Delta(^{18}O_2)$ = 23), and $\nu_{asym}$(Cu−O) = 497 $cm^{-1}$ ($\Delta(^{18}O_2)$ = 22) and suggest the $L^{ASM}$ ligand is a poorer electron donor to copper than is $L^{ESE}$. In contrast, the oxygenation of $[(L^{EOE})Cu^{I}]^{+}$ (**3a**), possessing an ether donor as an analogue of the thioether in $L^{ESE}$, led to the formation of a bis($\mu$-oxo) species $[\{(L^{EOE})Cu^{III}\}_2(O^{2-})_2]^{2+}$ (**3b$^{O}$**; 380 nm, $\varepsilon \sim 10{,}000$ $M^{-1}$ $cm^{-1}$). This result provides further support for the sulfur influence in **1b$^{P}$** and **2b$^{P}$**, in particular coordination of the sulfur to the Cu. Thermal decomposition of **1b$^{P}$** is accompanied by ligand sulfoxidation. The structure of $[\{(L^{EOE})Cu^{II}(Cl)\}_2]^{+}$ (**3c**) generated from the reductive dehalogenation of organic chlorides suggests that the ether moiety is weakly bound to the cupric ion. A detailed discussion of the spectroscopic and structural characteristics of **1b$^{P}$**, **2b$^{P}$**, and **3b$^{O}$** is presented.

## Introduction

Inspired by the known copper metalloprotein activities, copper mediated dioxygen activation studies employing a variety of organic ligands have focused on understanding the kinetics and thermodynamics of reactive intermediate formation and their diverse oxidative reactivity.[1−3] Previously, we have studied an end-on $\mu$-1,2-peroxo dicopper(II) intermediate with the tripodal tetradentate TMPA (tris(-2-pyridylmethyl)amine) ligand in terms of kinetics of formation, electronic structure, and other physical-spectroscopic properties, Scheme 1.[2,4,5]

**Scheme 1**

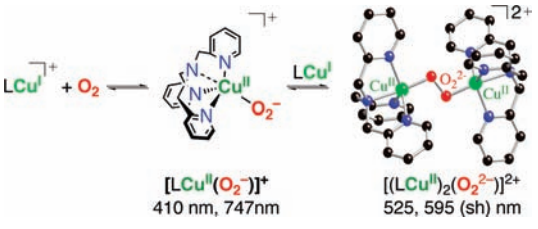


Detailed mechanistic studies revealed that $[\{(tmpa)Cu^{II}\}_2(O_2^{2-})]^{2+}$ formation occurs via a reversible reaction between

*To whom correspondence should be addressed. E-mail: karlin@jhu.edu.

(1) Hatcher, L. Q.; Karlin, K. D. *J. Biol. Inorg. Chem.* **2004**, *9*, 669–683.
(2) Mirica, L. M.; Ottenwaelder, X.; Stack, T. D. P. *Chem. Rev.* **2004**, *104*, 1013–1045.
(3) Lewis, E. A.; Tolman, W. B. *Chem. Rev.* **2004**, *104*, 1047–1076.


Published on Web 09/07/2010

a $Cu^{II}$-superoxo intermediate ($\lambda_{max}$ = 410 nm) with a second cuprous monomer, the equilibrium, however, lying far to the side of the binuclear complex.[6−8] The intensely purple [{(tmpa)$Cu^{II}$}$_2$($O_2^{2-}$)]$^{2+}$ species exhibits absorptions [$\lambda_{max}$ nm ($\varepsilon$ ($cm^{-1}$ $M^{-1}$))] at 440 (4,000), 525 (11,500), and 590 (7,600) nm in EtCN at −80 °C, assigned as ligand-to-metal charge-transfer (LMCT) transitions. The formulation as an end-on bound dioxygen adduct, at the peroxide level of reduction, was confirmed structurally (Scheme 1), with Cu···Cu = 4.359 Å and O−O = 1.432 Å, the latter value typical for peroxides.[4] Further confirmation came from resonance Raman spectroscopy, $\nu$(O−O) = 832 ($\Delta$($^{18}O_2$) = 44) $cm^{-1}$. Finally, a low energy d-d band (1035 nm; $\varepsilon$, 160) was observed, that is also consistent with the copper(II) formulation.

While the study of copper(I,II) and copper(I)/$O_2$ chemistry with ligands possessing all nitrogen donors is of continuing importance,[9−14] a complementary interest involves studies with thioether sulfur containing chelators for copper ions. In part, this relates to the (stereo)specific hydroxylation reactions of biological substrates which then function as neurotransmitters or hormones, those catalyzed by two closely related enzymes dopamine $\beta$-monooxygenase (D$\beta$M) and peptidylglycine α-hydroxylating monooxygenase (PHM), Figure 1.[15] Both enzymes are composed of a pair of noncoupled copper centers separated by ∼11 Å. The two sites have distinct functions. The first (called $Cu_H$ or $Cu_A$) is responsible for electron transfer and the second ($Cu_M$ or $Cu_B$) for $O_2$ activation near the substrate binding site.[16−18] The presence of mononuclear catalytic copper centers drive important questions regarding their proposed roles and reaction mechanism and contrasts to the binuclear mechanism in tyrosinase. PHM X-ray crystal structures reveal the catalytic copper center possesses (His-N)$_2$Met-S coordination. The role of the sulfur coordination has been hypothesized to allow PHM to utilize a mononuclear copper center to activate $O_2$ and perform hydroxylation reactions. Recently, a PHM structure has been solved with a slow substrate that shows an end-on bound dioxygen species as the possible active species in its substrate oxidation (Figure 1).[16] Two plausible

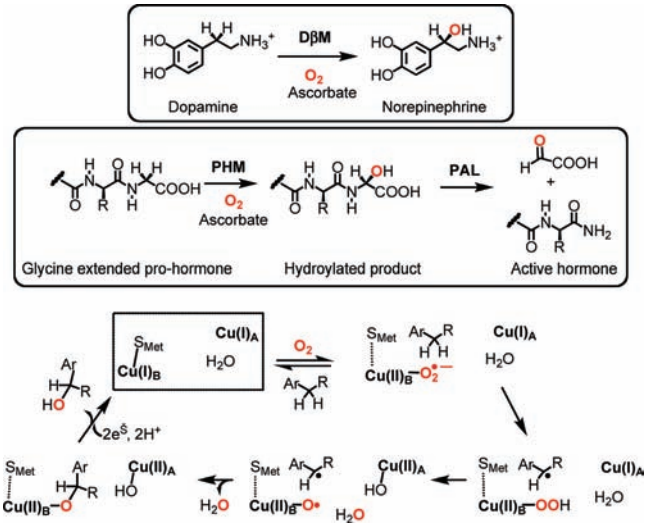


**Figure 1.** Enzymatic hydroxylations of substrates by D$\beta$M and PHM (top and middle) and one proposed mechanism of PHM and D$\beta$M (bottom). See text.

copper−oxygen species ($Cu^{II}$−OOH vs $Cu^{II}$($O_2^{-}$)) have been suggested as the initial hydrogen atom (H·) abstractor from the substrate in the proposed oxidation mechanisms; however, the nature of these species in terms of their oxidative reactivities are not well understood.[15,19−22] Figure 1 illustrates the mechanism suggested by Klinman, with a $Cu^{II}$-($O_2^{-}$) as active oxidant.[15,19] Some of us have also suggested a $Cu^{II}$-($O_2^{-}$) oxidant, albeit with an alternative substrate rebound mechanism.[20−22] Two specific details arising from the postulated mechanism are of considerable interest. First, the proposed involvement of a high-valent "cupryl" Cu−O species (by analogy to iron chemistry $Fe^{IV}$=O species) has been suggested (Figure 1) which would be expected to be a very potent oxidant itself and is intriguing from a coordination chemistry/bonding perspective.[23] Second, the presence of Met-S ligation in an oxygenation site is unusual in light of sulfur itself being susceptible to oxidation. Given the curiosity of such a donor ligand in these active sites, determination of the role of the Met-S and its electronic structure contributions to enzyme reactivity is warranted.

To these ends, we and other research groups (see Results and Discussion) have or are studying the chemistry of copper complexes with thioether containing ligands to assess the effect of sulfur coordination in biomimetic D$\beta$M and PHM complexes. In fact, we were able to describe the first example of a dioxygen adduct of copper ion employing an $N_3S$ donor set, in ligand $L^{ESE}$ and complex **2b**$^{\mathbf{P}}$ (Chart 1).[24] Spectroscopic analysis including UV−visible, resonance Raman, and extended X-ray absorption fine structure (EXAFS) spectroscopy indicated the formation of an end-on peroxo species [{($L^{ESE}$)$Cu^{II}$}$_2$($O_2^{2-}$)]$^{2+}$(**2b**$^{\mathbf{P}}$) akin to that found with the

(4) Jacobson, R. R.; Tyeklár, Z.; Karlin, K. D.; Liu, S.; Zubieta, J. *J. Am. Chem. Soc.* **1988**, *110*, 3690–3692.
(5) Tyeklár, Z.; Jacobson, R. R.; Wei, N.; Murthy, N. N.; Zubieta, J.; Karlin, K. D. *J. Am. Chem. Soc.* **1993**, *115*, 2677–2689.
(6) Karlin, K. D.; Kaderli, S.; Zuberbühler, A. D. *Acc. Chem. Res.* **1997**, *30*, 139–147.
(7) Zhang, C. X.; Kaderli, S.; Costas, M.; Kim, E.-i.; Neuhold, Y.-M.; Karlin, K. D.; Zuberbühler, A. D. *Inorg. Chem.* **2003**, *42*, 1807–1824.
(8) Fry, H. C.; Scaltrito, D. V.; Karlin, K. D.; Meyer, G. J. *J. Am. Chem. Soc.* **2003**, *125*, 11866–11871.
(9) Lee, Y.; Park, G. Y.; Lucas, H. R.; Vajda, P. L.; Kamaraj, K.; Vance, M. A.; Milligan, A. E.; Woertink, J. S.; Siegler, M. A.; Narducci Sarjeant, A. A.; Zakharov, L. N.; Rheingold, A. L.; Solomon, E. I.; Karlin, K. D. *Inorg. Chem.* **2009**, *48*, 11297–11309.
(10) Himes, R. A.; Karlin, K. D. *Curr. Opin. Chem. Biol.* **2009**, *13*, 119–131.
(11) Lucas, H. R.; Karlin, K. D. *Met. Ions Life Sci.* **2009**, *6*, 295–361.
(12) Sarangi, R.; York, J. T.; Helton, M. E.; Fujisawa, K.; Karlin, K. D.; Tolman, W. B.; Hodgson, K. O.; Hedman, B.; Solomon, E. I. *J. Am. Chem. Soc.* **2008**, *130*, 676–686.
(13) Itoh, S.; Fukuzumi, S. *Acc. Chem. Res.* **2007**, *40*, 592–600.
(14) Cramer, C.; Tolman, W. *Acc. Chem. Res.* **2007**, *40*, 601–608.
(15) Klinman, J. P. *J. Biol. Chem.* **2006**, *281*, 3013–3016.
(16) Prigge, S. T.; Eipper, B.; Mains, R.; Amzel, L. M. *Science* **2004**, *304*, 864–867.
(17) Prigge, S. T.; Mains, R. E.; Eipper, B. A.; Amzel, L. M. *Cell. Mol. Life Sci.* **2000**, *57*, 1236–1259.
(18) Prigge, S. T.; Kolhekar, A.; Eipper, B. A.; Mains, R. E.; Amzel, M. *Science* **1997**, *278*, 1300–1305.
(19) Evans, J. P.; Ahn, K.; Klinman, J. P. *J. Biol. Chem.* **2003**, *278*, 49691–49698.
(20) Chen, P.; Solomon, E. I. *J. Am. Chem. Soc.* **2004**, *126*, 4991–5000.
(21) Chen, P.; Bell, J.; Eipper, B. A.; Solomon, E. I. *Biochemistry* **2004**, *43*, 5735–5747.
(22) Chen, P.; Solomon, E. I. *Proc. Natl. Acad. Sci. U.S.A.* **2004**, *101*, 13105–13110.
(23) Decker, A.; Solomon, E. I. *Curr. Opin. Chem. Biol.* **2005**, *9*, 152–163.
(24) Hatcher, L. Q.; Lee, D.-H.; Vance, M. A.; Milligan, A. E.; Sarangi, R.; Hodgson, K. O.; Hedman, B.; Solomon, E. I.; Karlin, K. D. *Inorg. Chem.* **2006**, *45*, 10055–10057.

**Chart 1**

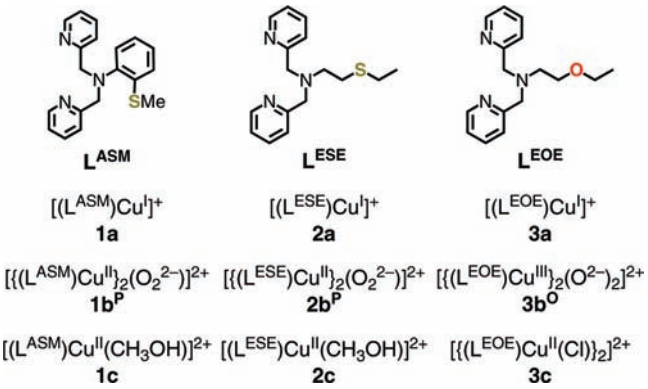


**Chart 2**

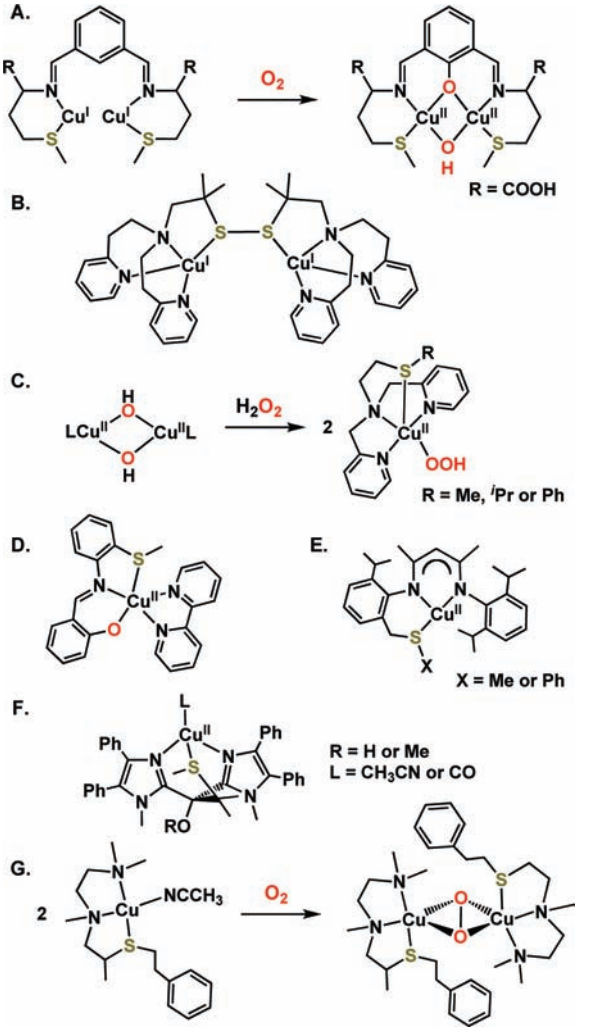


TMPA ligand, with the fourth ligand alkyl thioether sulfur also coordinated to the cupric ion.[24,25] In the present report, we describe the related ligand $L^{ASM}$ with thioanisole group and its $Cu^{I}/O_2$ chemistry to compare and contrast with the results obtained for $L^{ESE}$ (Chart 1). $L^{EOE}$ (Chart 2) with an ether oxygen donor instead of sulfur has also been synthesized for comparison with $L^{ESE}$. Peroxodicopper(II) complexes are found to be generated by the reaction of $O_2$ with **1** and **2**, while a bis($\mu$-oxo) complex forms by oxygenation of complex **3a** with the $L^{EOE}$ ligand (Chart 1). To appreciate the preferred structures of the Cu(II) ion in the coordination spheres of the new ligands, as well as to possibly relate such information to the coordination present in the peroxo complexes (**1b$^{P}$**)−(**3b$^{P}$**), copper(II) complexes (**1c**−**3c** in Chart 1) have been synthesized and characterized.

## Experimental Section

**General Considerations and Instrumentation.** All reagents and solvents used for this work were commercial products and are of reagent quality unless otherwise stated. Acetonitrile ($CH_3CN$), dichloromethane ($CH_2Cl_2$), diethylether ($Et_2O$), methanol ($CH_3OH$), and tetrahydrofuran (THF) were purified and dried by passing through a double alumina column solvent purification system by Innovative Technologies, Inc. Anhydrous 2-methyltetrahydrofuran (MeTHF; packaged under nitrogen in Sure/Seal bottles, 99+%) was purchased from Sigma-Aldrich, Inc. Deoxygenation of these solvents was achieved by bubbling Ar for 30 min and/or carrying out three freeze/pump/thaw cycles. Air-sensitive compounds were handled under an Ar atmosphere using standard Schlenk techniques or within a MBraun Labmaster 130 inert-atmosphere ($N_2$ atmosphere; < 1 ppm $O_2$, < 1 ppm $H_2O$) glovebox. Molecular oxygen (Airgas Inc., Radnor, PA) was dried by passing it through a laboratory gas drying unit (W. A. Hammond Drierite Co., Xenia, Ohio) and introduced to reaction solutions by bubbling through an 18-gauge, 24-in.-long stainless steel syringe needle. $[Cu^{I}(MeCN)_4]ClO_4$ and $[Cu^{I}(MeCN)_4]B(C_6F_5)_4$ were prepared by literature procedures.[26,27] $KB(C_6F_5)_4$ or $LiB(C_6F_5)_4$ were purchased from Boulder Scientific Company. $L^{ESE}$ and $[(L^{ESE})Cu^{I}]^{+}$ (**2a**) were prepared according to literature procedures.[24]

***Caution!*** *While we have experienced no problems in working with perchlorate compounds, they are potentially explosive, and care must be taken not to work with large quantities.*

**$^{1}$H NMR and $^{13}$C NMR** spectra were measured on a Varian 400 MHz or Bruker 400 MHz spectrometer and chemical shifts are reported in ppm ($\delta$) downfield from an internal TMS ($Me_4Si$) reference and the residual solvent proton peak. **Infrared Spectra** were recorded on a Mattson Instruments 4030 Galaxy Series FT-IR spectrometer. Measuring the solution IR spectra of carbonyl adducts (as a solution in THF) were recorded using standard solution IR cells. Air sensitive cuprous THF solutions were prepared in a glovebox ($N_2$ filled, MBraun) and then removed using 20 mL vials sealed with a 14/20 rubber septum. Carbon monoxide gas (Airgas Inc., Radnor, PA) was introduced to the corresponding solution via bubbling for 20−30 s through an 18-gauge, 24-in.-long stainless steel syringe needle. The resulting solution was transferred to a solution IR cell via a gastight syringe under the CO atmosphere. **Elemental Analyses** were performed by Desert Analytics, Tucson, AZ for air-sensitive samples or by Quantitative Technologies Inc. (QTI), Whitehouse, NJ for others. **Mass Spectrometry** was conducted at the mass spectrometry facility either at the Johns Hopkins University (JHU) or at The Ohio State University (OSU). Chemical Ionization (CI) and fast atomic bombardment (FAB) mass spectra were acquired at the JHU facility using a VG70S double focusing magnetic sector mass spectrometer (VG Analytical, Manchester, U.K., now Micromass/Wasters) equipped with a Xe gas FAB gun (8 kV @ 1.2 mA) and an off-axis electron multiplier and an MSS data system (MasCom, Bremen, Germany).

(25) Lee, D. H.; Hatcher, L. Q.; Vance, M. A.; Sarangi, R.; Milligan, A. E.; Narducci Sarjeant, A. A.; Incarvito, C. D.; Rheingold, A. L.; Hodgson, K. O.; Hedman, B.; Solomon, E. I.; Karlin, K. D. *Inorg. Chem.* **2007**, *46*, 6056–6068.

(26) Liang, H.-C.; Kim, E.; Incarvito, C. D.; Rheingold, A. L.; Karlin, K. D. *Inorg, Chem.* **2002**, *41*, 2209–2212.

(27) Liang, H.-C.; Karlin, K. D.; Dyson, R.; Kaderli, S.; Jung, B.; Zuberbühler, A. D. *Inorg. Chem.* **2000**, *39*, 5884–5894.

The resolution of the instrument was set at 10,000 (100 ppm peak width). Samples were mixed with *m*-nitrobenzyl-alcohol matrix deposited on the target of a direct insertion probe for introduction into the source. Nominal mass scan spectra were acquired with a mass scan range of 10−950 amu using a magnet scan rate of 25 s/dec For accurate mass measurements, a narrower mass scan range was employed, with the matrix containing 10% PEG mass calibrant. Electrospray ionization (ESI) mass spectra (JHU facility) were acquired using a Finnigan LCQDeca ion-trap mass spectrometer equipped with an electrospray ionization source (Thermo Finnigan, San Jose, CA). Samples were dissolved in $CH_3OH$ or $CH_3CN$ and introduced into the instrument at a rate of 10 $\mu l$/min using a syringe pump via a silica capillary line. The heated capillary temperature was 250 °C and the spray voltage was 5 kV. Fast atomic bombardment (FAB) mass spectra were acquired at the JHU facility using a VG70S double focusing magnetic sector mass spectrometer (VG Analytical, Manchester, U.K., now Micromass/Wasters) equipped with a Xe gas FAB gun (7.5 kV @ 1 mA) and an off-axis electron multiplier. High resolution ESI mass spectrometry analyses were performed at the OSU mass-spec facility with a 3-T Finnigan FTMS-2000 Fourier Transform mass spectrometer. Samples were sprayed from a commercial electrospray ionization source, and then focused into the FTMS cell using a home-built set of ion optics. **Electrical conductivity** measurements[28,29] for the Cu(I) complexes $[(L^{ASM})Cu^{I}]^{+}$ (**1a**) and $[(L^{ESE})Cu^{I}]^{+}$ (**2a**) were carried out in *N*,*N*-dimethylformamide (DMF) solvent using an Accumet AR20 pH/Conductivity meter (Fisher Scientific) with Accumet Immersion-type four-cell glass conductivity probe (cell constant $\kappa = 1.0\ cm^{-1}$). Air sensitive cuprous DMF solutions (1 mM, 20 mL) were prepared in a glovebox ($N_2$ filled, MBraun) and then removed using 5 drum vials sealed with a cap and electrical tape. The data were collected from measurements with continuous strong (over the top) Ar flow. **Cyclic voltammetry** measurements were undertaken in $CH_3CN$ and DMF using a BAS 100B electrochemical analyzer with a glassy carbon working electrode and a platinum wire auxiliary electrode. Potentials were recorded versus a $Ag/AgNO_3$ electrode. The voltammograms are plotted versus the $[Fe(Cp)_2]^{+/0}$ potential which was measured as an external standard.[30] Scans were run at 50−200 mV/s under an Ar atmosphere using about 0.1 M $[Bu_4N][PF_6]$ as the supporting electrolyte. **X-ray Crystallography** was performed on suitable single crystals of $[(L^{ASM})Cu^{I}]^{+}$ (**1a**), $[(L^{ASM})Cu^{II}(CH_3OH)]^{2+}$ (**1c**), and $[\{(L^{EOE})Cu^{II}(Cl)\}_2]^{2+}$ (**3c**), which were mounted in Paratone-N oil on the end of a glass fiber and transferred to the $N_2$ cold stream (110 K) of an Oxford Diffraction Xcalibur3 system equipped with Enhance optics [Mo Ka radiation ($\lambda = 0.71073$ Å)] and a CCD detector. The frames were integrated and a face indexed absorption correction, and an interframe scaling correction was also applied with the Oxford Diffraction CrysAlisRED software package (CrysAlis CCD, Oxford Diffraction Ltd., Version 1.171.27p5 beta). The structures were solved using direct methods and refined using the Bruker SHELXTL (v6.1) software package. **Resonance Raman** spectra were obtained using a Princeton Instruments ST-135 back-illuminated CCD detector on a Spex 1877 CP triple monochromator with 1200, 1800, and 2400 grooves/mm holographic spectrograph gratings. Excitation was provided by a Coherent I90C-K $Kr^+$ ion laser. The laser line, 568 nm (~10 mW), was chosen to coincide with the intense absorption transition of the $Cu_2O_2$ species. The spectral resolution was $< 2\ cm^{-1}$. Sample concentrations were approximately 3−4 mM with respect to Cu (1.5−2 mM with respect to dimer). The samples were cooled to 77 K in a quartz liquid nitrogen finger Dewar (Wilmad) and rotated by hand to minimize sample decomposition during scan collection. Isotopic substitution was achieved by oxygenation with $^{18}O_2$. **X-Band Electron Paramagnetic Resonance (EPR) Spectra** were recorded on a Bruker EMX CW-EPR spectrometer controlled with a Bruker ER 041 XG microwave bridge operating at X-band (~9 GHz). The low-temperature experiments were carried out via either a continuous-flow He(*l*) cryostat and ITC503 temperature controller made by Oxford Instruments, Inc. or an $N_2(l)$ finger dewar. **Low Temperature UV−vis Spectra** were obtained with either a Cary 50 Bio spectrophotometer equipped with a fiber optic coupler (Varian) and a fiber optic dip probe (Hellma: 661.302-QX-UV-2 mm for low temperature) or a Hewlett-Packard model 8453 diode array spectrophotometer equipped with a custom-made quartz-windowed vacuum dewar filled with methanol (−80 °C). A low temperature unit (Neslab ULT-95 low temperature circulator) is attached to the HP spectrophotometer via copper tubing. The methanol temperature within the dewar was monitored using a thermocouple probe (Omega Model 651). For the low temperature measurements with a Cary 50 Bio spectrophotometer, a hexane/$N_2(l)$ bath (−94 °C) or a pentane/$N_2(l)$ bath (−128 °C) was used, and the steady temperature was monitored with the type T thermocouple thermometer (Model 650, Omega engineering, CT). Air sensitive solutions were prepared in a glovebox ($N_2$ filled, MBraun) and carried out in custom-made Schlenk tubes designed for the dip probe (Chemglass: JHU-0407−271MS) or Schlenk cuvettes. The cuvette assembly consisted of a two-window quartz cuvette (2 mm path) connected, via a 12 cm glass tube, to a 14/20 female ground glass joint.

**Synthesis of Ligands.** $L^{ASM}$**.** The compound 2-(methylthio)-aniline (2.05 g, 14.0 mmol) and picolyl chloride hydrochloride (7.25 g, 44.4 mmol) were dissolved in DMF (100 mL). Sodium hydride (3.8 g, 60% dispersion in mineral oil, 95.0 mmol) was slowly introduced with vigorous stirring in the precooled (ice bath) solution. The reaction mixture was refluxed for 6 h under Ar. After cooling to room temperature, ethanol (20 mL) was added to quench the unreacted sodium hydride. The resulting solution was filtered, and DMF was removed by rotary evaporation. The crude yellow oil was dissolved in $CH_2Cl_2$ and washed three times with brine. The organic layer was separated, dried over anhydrous $MgSO_4$, then filtered and concentrated under vacuum. The yellow powder obtained (2.2 g, 6.9 mmol, 49.3%) was purified by column chromatography (Silica gel, ethylacetate, $R_f = 0.2$). $^1H$ NMR ($CDCl_3$): $\delta$ 8.47 (d, $J = 4$ Hz, 2H), 7.65 (d, $J = 7.8$ Hz, 2H), 7.59 (td, $J = 7.6, 1.8$ Hz, 2H), 7.1 (m, 5H), 6.97 (td, $J = 7.3, 1.8$ Hz, 1H), 4.38 (s, 4H), 2.47 (s, 3H). $^{13}C$ NMR ($CDCl_3$): $\delta$ 158.5 (Py), 148.4 (Py), 146.3 (Py), 136.1 (Ar), 135.7 (Ar), 124.6 (Py), 124.1 (Ar), 123.5 (Ar), 122.2 (Ar), 122.0 (Py), 121.6 (Py), 59.0 ($NCH_2$), 13.8 ($CH_3$). FAB mass spectrum: $m/z$ 322.2 $(M + 1)^+$.

$L^{EOE}$**.** Bis((pyridin-2-yl)methyl)amine (PY**1**) (3.05 g, 15.0 mmol) and 2-chloroethyl ethyl ether (2.41 g, 22.2 mmol) were dissolved in methanol (100 mL). After potassium hydroxide (1.5 g, 26.7 mmol) was introduced, the reaction mixture was refluxed overnight under Ar. After cooling to room temperature, the resulting solution was filtered and solvent was removed by rotary evaporator. The crude yellow oil was dissolved in $CH_2Cl_2$ and washed with brine three times. The organic layer was separated, dried over anhydrous $MgSO_4$, filtered and concentrated under vacuum. The oil obtained was purified by column chromatography (Silica gel, ethylacetate, $R_f = 0.3$). Yield is 0.388 g (1.43 mmol, 95%). $^1H$ NMR ($CDCl_3$): $\delta$ 8.52 (d, $J = 4$ Hz, 2H), 7.64 (td, $J = 7.4, 1.8$ Hz, 2H), 7.57 (d, $J = 7.8$ Hz, 2H), 7.13 (t, $J = 5.1$ Hz, 2H), 3.91 (s, 4H), 3.58 (t, $J = 6$ Hz, 2H), 3.43 (q, $J = 7$ Hz, 2H), 2.83 (t, $J = 6$ Hz, 2H), 1.17 (t, $J = 7.2$ Hz, 3H). $^{13}C$ NMR ($CDCl_3$): $\delta$ 160.1 (py), 149.1 (py), 136.5 (py), 123.0 (py), 122.0 (py), 69.0 ($OCH_2$), 66.5 ($OCH_2$), 61.1 ($NCH_2$), 53.9 ($NCH_2$), 15.4 ($CH_3$). FAB mass spectrum: $m/z$ 322.2 $(M + 1)^+$.

**Synthesis of Cu(I) Complexes and Their Reactivity toward** $O_2$**.** $[(L^{ASM})Cu^{I}]B(C_6F_5)_4$ **(1a·B(C$_6$F$_5$)$_4$).** $L^{ASM}$ (0.26 g, 0.8 mmol) and $[Cu^{I}(CH_3CN)_4]B(C_6F_5)_4$ (0.682 g, 0.75 mmol) were dissolved and stirred for 1 h in $O_2$-free THF (15 mL) under Ar at room temperature. The resulting yellow solution was filtered and transferred to a 100 mL Schlenk flask by cannula (with filter paper).

(28) Geary, W. J. *Coord. Chem. Rev.* **1971**, *7*, 81–122.
(29) Sorrell, T. N.; Borovik, A. S. *J. Am. Chem. Soc.* **1987**, *109*, 4255–4260.
(30) Connelly, N. G.; Geiger, W. E. *Chem. Rev.* **1996**, *96*, 877–910.

The complex precipitated as a yellow powder upon addition of $O_2$-free heptane into the reaction mixture. The supernatant was decanted, and the resulting yellow powder (0.55 g, 0.52 mmol, 70%) was washed two times with $O_2$-free heptane and dried under vacuum. $^1$H NMR ($CD_2Cl_2$): $\delta$ 8.85 (s, 2H), 7.80 (m, 4H), ~ 7.5 (m, 6H), ~ 4.6(s, 4H), 2.5 (s, 3H), 2.18 (s, $CH_3CN$). Anal. Calcd. for $C_{43}H_{19}BCuF_{20}N_3S(1/4CH_3CN)$: C, 48.63; H, 1.85; N, 4.24. Found: C, 48.47; H, 1.69; N, 4.24. ESI mass spectrum: $m/z$ 384.35 $(LCu^I)^+$. UV−vis (MeTHF; $\lambda_{max}$, nm; $\varepsilon$, $M^{-1}$ $cm^{-1}$): 318;5100.

**$[(L^{ASM})Cu^I]ClO_4$ (1a·ClO$_4$).** $L^{ASM}$ (0.500 g, 1.6 mmol) and $[Cu^I(CH_3CN)_4]ClO_4$ (0.51 g, 1.6 mmol) were dissolved and stirred for 1 h in $O_2$-free $CH_3CN$ (15 mL) under Ar at room temperature. The resulting yellow solution was filtered and transferred to a 100 mL Schlenk flask by cannula (with filter paper). The complex precipitated as a yellow powder upon addition of $O_2$-free diethylether and heptane into the reaction mixture. The supernatant was decanted, and the resulting yellow powder (0.57 g, 1.2 mmol, 75%) was washed two times with $O_2$-free ether/heptane and dried under vacuum. $^1$H NMR (DMSO-$d_6$): $\delta$ 8.66 (d, $J$ = 4.4 Hz, 2H), 7.87 (td, $J$ = 8, 1 Hz, 4H), ~ 7.4 (m, 6H), ~ 4.3 (s, 4H), 2.5 (s, 3H), 2.11 (s, $CH_3CN$). Anal. Calcd. for $C_{19}H_{19}ClCuN_3O_4S(1/3CH_3CN)$: C, 47.42; H, 4.05; N, 9.37. Found: C, 47.11; H, 4.06; N, 9.25. ESI mass spectrum: $m/z$ 384.14 $(LCu^I)^+$.

**$[(L^{EOE})Cu^I]^+$ (3a).** $L^{EOE}$ (75 mg, 0.28 mmol) and $[Cu^I(CH_3CN)_4]B(C_6F_5)_4$ (245 mg, 0.27 mmol) were stirred for 1 h in $O_2$-free THF (5 mL) under Ar at room temperature (RT). The complex was precipitated as yellowish white powder upon addition of (oxygen free) heptane into the reaction mixture. The supernatant was decanted. The resulting yellow powder was washed two times with $O_2$-free heptane and dried under vacuum. $^1$H NMR ($CD_3NO_2$): $\delta$ 9.08 (s, 4H), 7.97 (s, 2H), 7.56 (s, 1H), 7.37 (s, 1H), 5.42 (s, 4H), 4.56 (s, 2H), 2.85 (s, 2H), 2.29 (s, 2H), 1.28 (s, 3H). Anal. Calcd. for $C_{40}H_{21}BCuF_{20}N_3O$: C, 47.38; H, 2.09; N, 4.14. Found: C, 47.04; H, 2.46; N, 4.10. ESI mass spectrum: $m/z$ 334.57 $(LCu^I)^+$. UV−vis (THF; $\lambda_{max}$, nm; $\varepsilon$, $M^{-1}$ $cm^{-1}$): 330; 4,300.

**$L^{AS(O)M}$ Formation.** $[(L^{ASM})Cu^I]^+$ (**1a**) (0.13 g, 0.12 mmol) was dissolved in $O_2$-free THF (5 mL) under Ar in a 25 mL Schlenk flask. While $O_2$ gas was bubbling through the yellow solution (~2 min) at −77 °C, it turned deep blue corresponding to peroxo species $[\{(L^{ASM})Cu^{II}\}_2(O_2^{2-})]^{2+}$ (**1b$^P$**). This solution was then slowly warmed and stirred overnight at room temperature. The solvent was removed by rotary evaporation and the residual green material was demetalated with $NH_4OH$/$CH_2Cl_2$.[31,32] The organic layer was separated, washed three times with brine, dried over anhydrous $MgSO_4$, then filtered and concentrated under vacuum. The resulting yellow powder was purified by column chromatography ($Al_2O_3$, ethylacetate, $R_f$ = 0.13) to give 15 mg (0.045 mmol, 37%) product. $^1$H NMR ($CDCl_3$) $\delta$: 8.53 (dm, $J$ = 4.4 Hz, 2H), 7.93 (dd, $J$ = 7.2, 1.8 Hz, 1H), 7.60 (td, $J$ = 7.6, 2.1 Hz, 2H), ~ 7.3 (m, 4H), ~ 7.2 (m, 3H), 4.39 (ABq, $J$ = 14.5 Hz, 4H), 2.90 (s, 3H). $^{13}$C NMR ($CDCl_3$): $\delta$ 157.1 (Py), 149.0 (Py), 147.4 (Py), 141.1 (Ar), 136.1 (Ar), 130.9 (Py), 125.3 (Ar), 124.1 (Ar), 123.1 (Ar), 122.9 (Py), 122.1 (Py), 60.0 ($NCH_2$), 42.1 ($CH_3$). FAB mass spectrum: $m/z$ 338.1 $(M + 1)^+$.

**$L^{AS(18O)M}$ Formation: $^{18}O_2$ Labeling Experiment.** $[(L^{ASM})Cu^I]^+$ (**1a**) (0.092 g, 0.086 mmol) was dissolved in $O_2$-free THF (5 mL) under Ar in a 25 mL Schlenk flask connected to a three-way valve, and a vacuum was applied and an $^{18}O_2$ bulb (25 mL, 99 atom %, 1 atm from ICON, part number IO 6393) was connected. At RT, dioxygen $^{18}O_2$ was allowed to diffuse into the reaction flask after breaking the seal. The reaction solution was stirred overnight, and the aliquot of reaction mixture was taken out for the mass spectrometric analysis. ESI mass data: Calculated values for $C_{19}H_{19}CuN_3(^{18}O)S$ with 92% incorporation of $^{18}O$: 400 (8.3%), 401 (1.9%), 402 (100%), 403 (22.6%), 404 (49.6%), 405 (10.8%), 406 (3.1%), 407 (0.5%). Found: 400 (4.8%), 401 (9.6%), 402 (100.0%), 403 (27.2%), 404 (49.6%), 405 (12.1%), 406 (3.5%), 407 (0.5%). After the solvent was removed in vacuo, the residual green material was treated with $NH_4OH/CH_2Cl_2$ to demetallate the resulting product.[31,32] The organic layer was separated, washed with brine (3 times), dried over anhydrous $MgSO_4$, then filtered and concentrated under vacuum. Thin layer chromatography (TLC) and NMR spectroscopy were used to confirm the purity and identity of the sulfoxide product. Subsequent mass spectrometric analysis indicated a 92% incorporation of the labeled oxygen. FAB mass data: Calculated values for $C_{19}H_{19}CuN_3(^{18}O)S$ with 92.5% incorporation of $^{18}O$: 338 (8.1%), 339 (1.8%), 340 (100%), 341 (22.7%), 342 (6.9%), 343 (1.2%). Found: 338 (8.24%), 339 (5.29%), 340 (100%), 341 (22.3%), 342 (7.5%), 343 (1.6%).

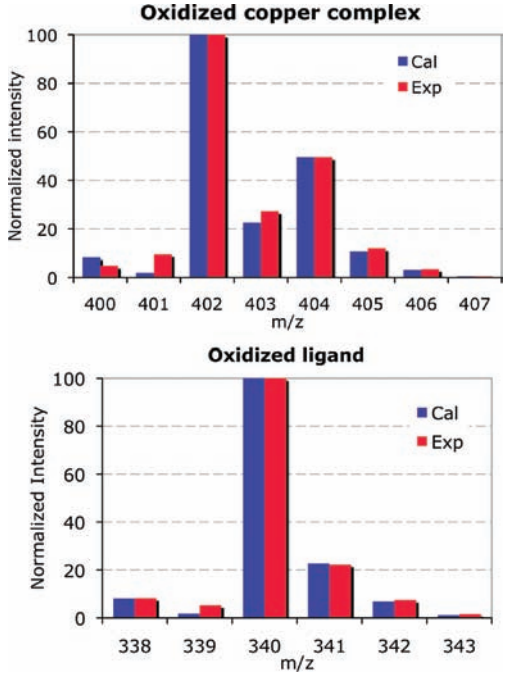


ESI mass data of oxidized copper complex shows 92% $^{18}O$ incorporation (left) and FAB mass data of the oxidized ligand shows 92.5% $^{18}O$ incorporation (right). Blue bars represent calculated values and red bars represent experimental values.

**Synthesis and Characterization of Cu(II) Complexes. $[(L^{ASM})Cu^{II}(CH_3OH)]^{2+}$ (1c).** $L^{ASM}$ (0.45 g, 1.4 mmol) and $Cu^{II}(ClO_4)_2 \cdot 6H_2O$ (0.52 g, 1.4 mmol) were dissolved in $CH_3OH$ (5 mL) and stirred for 1 h at room temperature. The resulting blue solution was filtered and transferred to a 100 mL Schlenk flask by cannula (with filter paper). The solution was layered with diethylether and crystallization/precipitation slowly took place in a refrigerator. After the supernatant was decanted, the resulting powder was washed two times with diethylether and dried under vacuum to give 0.79 g (1.29 mmol, 74%) product. UV−vis ($CH_3OH$; $\lambda_{max}$, nm; $\varepsilon$, $M^{-1}$ $cm^{-1}$): 256, 12,700; ~ 400, ~ 70; 710, 76. Anal. Calcd. for $C_{19}H_{21}Cl_2CuN_3O_9S(1/2\ H_2O)$: C, 37.35; H, 3.63; N, 6.88. Found: C, 37.41; H, 3.57; N, 6.70. EPR: X-band spectrometer ($\nu$ = 9.186 GHz) in 2-methyltetrahydrofuran/$CH_3CN$ (1:1) at 77 K; $g_{\|}$ = 2.28, $A_{\|}$ = 158 gauss; $g_{\perp}$ = 2.06. X-ray quality blue crystals were obtained from this synthesis.

(31) Karlin, K. D.; Nasir, M. S.; Cohen, B. I.; Cruse, R. W.; Kaderli, S.; Zuberbühler, A. D. *J. Am. Chem. Soc.* **1994**, *116*, 1324–1336.
(32) Sanyal, I.; Mahroof-Tahir, M.; Nasir, S.; Ghosh, P.; Cohen, B. I.; Gultneh, Y.; Cruse, R.; Farooq, A.; Karlin, K. D.; Liu, S.; Zubieta, J. *Inorg. Chem.* **1992**, *31*, 4322–4332.

$[\{(L^{EOE})Cu^{II}(Cl)\}_2]^{2+}$ (**3c**). **3a**·$B(C_6F_5)_4$ (40 mg, 0.039 mmol) was dissolved in $CH_2Cl_2$ (3 mL) and stirred for 30 min at room temperature under Ar. The blue solid was slowly precipitated out and supernatant was decanted by cannula (with filter paper). The resulting powder was washed two times with $CH_2Cl_2$ and dried under vacuum to give 38 mg (0.036 mmol, 92%) product. UV−vis ($CH_3CN$; $\lambda_{max}$, nm; $\varepsilon$, $M^{-1}$ $cm^{-1}$): 679; 58. ESI mass spectrum: $m/z$ 369.31 $(LCu^I)^+$. Anal. Calcd. for $C_{41}H_{23}BCl_3CuF_{20}N_3O$: C, 43.41; H, 2.04; N, 3.70. Found: C, 43.22; H, 2.23; N, 3.66. X-ray quality blue crystals were obtained from **3a** THF/$CH_2Cl_2$ solution layered with pentane.

## Results and Discussion

**Previously Studied Systems.** Copper complexes with thioether containing ligands have long been of interest because of their occurrence at electron-transfer sites in Type 1 "blue" copper proteins. There, studies focused on determination of the effects of RSR′ coordination upon redox and/or structural properties.[33−35] Here, as background literature, we highlight investigations of copper complexes with thioether ligands which have been directed toward chemistries of possible relevance to D$\beta$M and PHM (see Introduction) oxidative reactivity.

Casella and co-workers[36] reported that C−H bond activation with molecular oxygen and mediated by a dicopper complex could occur utilizing thioether containing ligands (**A**, Chart 1). This aromatic hydroxylation, which is reminiscent to previously studied xylyl systems in our lab,[31,37,38] was observed as monooxygenase type chemistry; a sulfoxide was detected as a minor fraction of the reacted ligand (15−20%).[36] Similar sulfoxidation chemistry was carried out by Reglier and co-workers[39] from the reactions of a copper(II) complex with hydrogen peroxide. However, no superoxo copper(II) ($Cu^{II}-O_2^{\bullet-}$) or hydroperoxo copper(II) ($Cu^{II}-OOH$) intermediates were detected. Reacting $H_2O_2$ with sulfur containing complexes **B** and **C** (R = $C_6H_5$, or $-CH_3$ or iso-$C_3H_7$), resulted in the detection of sulfoxide and sulfone products, and hydroperoxo copper(II) ($Cu^{II}-OOH$) complexes were generated and studied (Chart 1).[40,41] Santra and co-workers[42] reported a structural model for the oxidized $Cu_M$ site of D$\beta$H and PHM; $N_3OS$ copper(II) complex **D** is an example where thioether coordination occurs in the axial position. Tolman and co-workers[43] reported a $Cu^I/O_2$ reactivity study using a $\beta$-diketiminate thioether $N_2S-Cu(I)$ complex (**E**, Chart 1); the thioether donor does not seem to influence formation of mononuclear $Cu-O_2$ or dinuclear bis-$\mu$-oxo dicopper(III) products; for the latter, the R-S-X donor does not bind to the copper ion. Zhou and co-workers showed the oxygenation chemistry of a imidazolyl $N_2S$-copper(I) complex (R = H, L = $CH_3CN$, **F**, Chart 1) led to a 20% yield of a sulfoxidation product.[44] More recently, these same researchers generated a series of ligands similar to **F**, but with different R groups (including R = H) and varying substituents on the S-atom (e.g., -*t*Bu, -trityl); resulting (ligand)-$Cu^I/O_2$ reactivity studies led to a variety of product types, including dialkoxo and dihydroxo bridged dicopper(II) complexes, ligand hydroxylated species, and ligand disulfide products (following detritylation chemistry).[45] Most recently, we reported on the reaction depicted in **G**, a new structural type, that is, a $\mu$-$\eta^2$:$\eta^2$-peroxodicopper(II) complex which includes a thioether ligand donor.[46] In spite of all these known chemistries, studies systematically interrogating the direct influence of sulfur coordination on copper-dioxygen complex formation are rare.

**Synthesis of New Ligands and Copper(I) Complexes.** Ligands $L^{ASM}$ and $L^{EOE}$ and their copper complexes were synthesized and characterized. $L^{ASM}$ was prepared by reaction of 2-(methylthio)aniline with picolyl chloride and base. The ether ligand $L^{EOE}$ was generated from the reaction of bis((pyridin-2-yl)methyl)amine (PY1) and 2-chloroethyl ethyl ether under basic conditions (Scheme 2).

**Scheme 2**

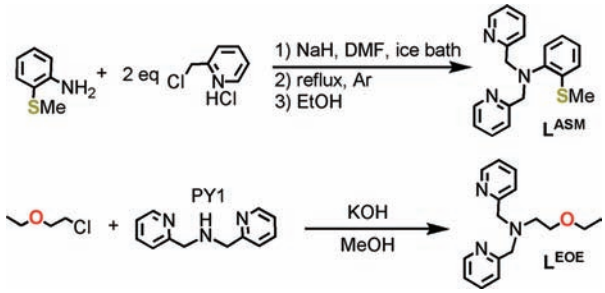


$[(L^{ASM})Cu^I]^+$ (**1a**) and $[(L^{EOE})Cu^I]^+$ (**3a**) were synthesized by the addition of 1 equiv of the appropriate tripodal ligand to $[Cu^I(CH_3CN)_4]Y$ (Y = $ClO_4^-$, $B(C_6F_5)_4^-$) in $CH_3CN$ or THF under Ar. They are both yellow, possessing charge-transfer absorptions at 318 and 330 nm respectively (see the Experimental Section and figures below). $^1H$ NMR and elemental analysis of **1a** indicate that the complex is consistently isolated with a less than a stoichiometric amount of $CH_3CN$. Solution conductivity measurements in DMF solvent indicate 1:1 electrolyte behavior for both $[(L^{ASM})Cu^I]^+$ (**1a**) and $[(L^{ESE})Cu^I]^+$ (**2a**) ($\Lambda_M$ = 77 and 78 ohm$^{-1}$ cm$^2$ mole$^{-1}$, respectively), consistent with their mononuclear formulations in this solvent.[28] While **2a** is a dimer in the solid state (formed by having one pyridyl group on each copper-ligand moiety coordinate to the other copper-ligand group),[25] **1a** crystallizes as a mononuclear species (Figure 2 and Table 1). This observation is most likely due to the structural rigidity of the

(33) Rorabacher, D. B. *Chem. Rev.* **2004**, *104*, 651–697.
(34) Ambundo, E. a.; Yu, Q. Y.; Ochrymowycz, L. A.; Rorabacher, D. B. *Inorg. Chem.* **2003**, *42*, 5267–5273.
(35) Karlin, K. D.; Yandell, J. K. *Inorg. Chem.* **1984**, *23*, 1184–1188.
(36) Alzuet, G.; Casella, L.; Villa, M. L.; Carugo, O.; Gullotti, M. *J. Chem. Soc., Dalton Trans.* **1997**, 4789–4794.
(37) Nasir, M. S.; Cohen, B. I.; Karlin, K. D. *J. Am. Chem. Soc.* **1992**, *114*, 2482–2494.
(38) Pidcock, E.; Obias, H. V.; Zhang, C. X.; Karlin, K. D.; Solomon, E. I. *J. Am. Chem. Soc.* **1998**, *120*, 7841–7847.
(39) Champloy, F.; Benali-Cherif, N.; Bruno, P.; Blain, I.; Pierrot, M.; Reglier, M.; Michalowicz, A. *Inorg. Chem.* **1998**, *37*, 3910–3918.
(40) Ohta, T.; Tachiyama, T.; Yoshizawa, K.; Yamabe, T.; Uchida, T.; Kitagawa, T. *Inorg. Chem.* **2000**, *39*, 4358–4369.
(41) Kodera, M.; Kita, T.; Miura, I.; Nakayama, N.; Kawata, T.; Kano, K.; Hirota, S. *J. Am. Chem. Soc.* **2001**, *123*, 7715–7716.
(42) Santra, B. K.; Reddy, P. A. N.; Nethaji, M.; Chakravarty, A. R. *Inorg. Chem.* **2002**, *41*, 1328–1332.
(43) Aboelella, N. W.; Gherman, B. F.; Hill, L. M. R.; York, J. T.; Holm, N.; Young, V. G.; Cramer, C. J.; Tolman, W. B. *J. Am. Chem. Soc.* **2006**, *128*, 3445–3458.
(44) Zhou, L.; Powell, D.; Nicholas, K. M. *Inorg. Chem.* **2006**, *45*, 3840–3842.
(45) Zhou, L.; Powell, D.; Nicholas, K. M. *Inorg. Chem.* **2007**, *46*, 7789–7799.
(46) Park, G. Y.; Lee, Y.; Lee, D.-H.; Woertink, J. S.; Sarjeant, A. A. N.; Solomon, E. I.; Karlin, K. D. *Chem. Commun.* **2010**, *46*, 91–93.

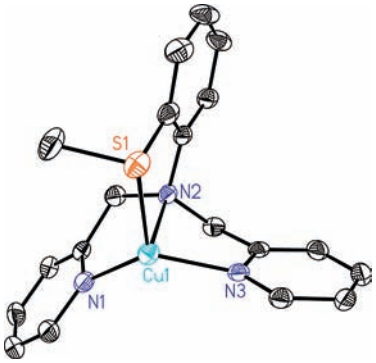


**Figure 2.** Molecular structure of the isolated cation $[(L^{ASM})Cu^{I}]^{+}$ (**1a-B($C_6F_5$)$_4$**) from X-ray crystallographic analysis. The $B(C_6F_5)_4^{-}$ counteranion and hydrogen atoms in the ORTEP view are omitted for clarity.

**Table 1.** Selected Bond Distances and Angles for $[(L^{ASM})Cu^{I}]^{+}$ (**1a-B($C_6F_5$)$_4$**)

| Cu−X | bond distance (Å) | X−Cu−X | bond angle (deg) |
|---|---|---|---|
| | | N(3)−Cu(1)−N(1) | 128.60 (9) |
| Cu(1)−S(1) | 2.26858 (8) | N(3)−Cu(1)−N(2) | 83.37 (8) |
| Cu(1)−N(1) | 2.027 (2) | N(1)−Cu(1)−N(2) | 83.90 (8) |
| Cu(1)−N(2) | 2.181 (2) | N(3)−Cu(1)−S(1) | 120.94 (6) |
| Cu(1)−N(3) | 1.990 (2) | N(1)−Cu(1)−S(1) | 108.01 (6) |
| | | N(2)−Cu(1)−S(1) | 87.71 (6) |

ligand in **1a** which prohibits its dimerization. In contrast, the thioether sulfur atom in **2a** is flexible and coordinates to the "other" copper ion.[25] The Cu−S distance (2.26858 (8) Å) in **1a** is slightly longer than that for **2a** (2.2023(9) Å) suggesting that the dimerization leading to **2a** allows the sulfur atom to bind to copper more tightly and that the thioanisole group in **1a** is a poorer donor than the alkyl thioether ligand. In **1a**, the Cu(I) is pushed out of the N1N3S1 plane (away from N2) by 0.206 Å. The angle between the N1N3S1 plane and the Cu1N2S1 plane is 88.9°. The structure of **1a** shows the copper(I) ion is out from the center of ligand coordination environment forming a distorted tetrahedral geometry, suggestive of its facile $O_2$ reactivity, vide infra.

**Copper(I) Complex Carbon Monoxide Binding.** To obtain insights into the solution state structures of these copper(I) complexes, as well as to obtain information concerning the relative amount of electron donation to the copper(I) ion as a function of ligand set (i.e., TMPA vs $L^{ASM}$ vs $L^{ESE}$ vs $L^{EOE}$), (ligand)$Cu^{I}$−CO complexes were generated and IR spectra were recorded. We have previously used CO-adducts for such purposes when studying a variety of copper(I) complexes with either tridentate or tetradentate ligands, and possessing systematically varied pyridyl 4-substituents.[7,24] In general, copper(I)-CO complexes have been widely studied,[47−53] including to compare/contrast to copper protein carbonyl adducts.[29,54]

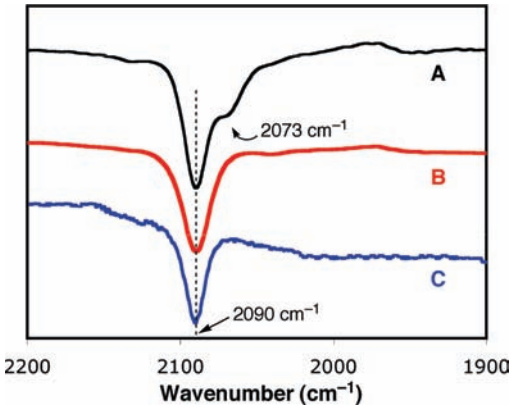


**Figure 3.** Solution IR spectra of copper(I) carbonyl complexes (**A**: [(tmpa)$Cu^{I}$(CO)]$^{+}$, **B**: **1a**-CO and **C**: **3a**-CO) in THF at room temperature. See Table 2 for $\nu$(C−O) values.

**Table 2.** Carbonyl Stretching Frequencies for Copper(I) Carbonyl Complexes in THF

| compound | wavenumber ($cm^{-1}$) |
|---|---|
| $[(tmpa)Cu^{I}(CO)]^{+}$ | 2090, 2073 |
| $[(PY1)Cu^{I}(CO)]^{+}$[55] | 2091[a] |
| $[(L^{ASM})Cu^{I}(CO)]^{+}$ | 2090 |
| $[(L^{ESE})Cu^{I}(CO)]^{+}$[25] | 2094[a] |
| $[(L^{EOE})Cu^{I}(CO)]^{+}$ | 2090 |

[a] Measured in $CH_3CN$.

With appropriate ligands (TMPA, $L^{ASM}$, and $L^{EOE}$) Cu(I)-CO species as $B(C_6F_5)_4$ complex salts were obtained by bubbling carbon monoxide gas into the corresponding THF solution at room temperature. The two bands observed at 2090 and 2073 $cm^{-1}$ seen for [(tmpa)$Cu^{I}$(CO)]$^{+}$ (Figure 3) have been previously attributed to a dynamic equilibrium involving overall 4- or 5-coordinate complexes, as illustrated in Scheme 3 [Note: formulations with superscripted **4c** indicate a complex with overall tetracoordination, while a superscripted **5c** indicates overall pentacoordination].[5,55,56] The lower value is ascribed to the pentacoordinate species where ligation of all four N-donors provides more electron density to the Cu(I) ion, resulting in greater back-donation to the CO $\pi^*$ orbital (thus weakening the CO bond and lowering $\nu$(C−O)). Supporting evidence comes from the observation that a Cu(I)-CO-complex with the tridentate PY1 ligand (see Scheme 3) gives a $\nu$(C−O) = 2091 $cm^{-1}$.[55] As reported for $L^{ESE}$,[24,25] the copper(I)-CO complex with $L^{ASM}$ gives only one IR peak (Figure 3, A), at 2090 $cm^{-1}$, the same as that for the 4-coordinated ($N_3$-ligated) TMPA complex (Scheme 3). Thus, we can conclude that the thioether donor in $[(L^{ASM})Cu^{I}(CO)]^{+}$ $^{4c}$(**1a-CO**) is not ligated. Similarly, $[(L^{EOE})Cu^{I}(CO)]^{+}$ $^{4c}$(**3a-CO**), does not possess a ligated ether oxygen donor (Figure 3, C; Scheme 3).

**Electrochemical Behavior of Copper(I) Complexes.** The electrochemical characteristics of $[(L^{ASM})Cu^{I}]^{+}$ (**1a**) were

(47) Osako, T.; Terada, S.; Tosha, T.; Nagatomo, S.; Furutachi, H.; Fujinami, S.; Kitagawa, T.; Suzuki, M.; Itoh, S. *Dalton Trans.* **2005**, 3514–3521.
(48) Pasquali, M.; Marini, G.; Floriani, C.; Gaetanimanfredotti, A.; Guastini, C. *Inorg. Chem.* **1980**, *19*, 2525–2531.
(49) Jonas, R. T.; Stack, T. D. P. *Inorg. Chem.* **1998**, *37*, 6615–6629.
(50) Kitajima, N.; Fujisawa, K.; Fujimoto, C.; Moro-oka, Y.; Hashimoto, S.; Kitagawa, T.; Toriumi, K.; Tatsumi, K.; Nakamura, A. *J. Am. Chem. Soc.* **1992**, *114*, 1277–1291.
(51) Dias, H. V. R.; Lovely, C. J. *Chem. Rev.* **2008**, *108*, 3223–3238.
(52) Kealey, S.; Miller, P. W.; Long, N. J.; Plisson, C.; Martarello, L.; Gee, A. D. *Chem. Commun.* **2009**, 3696–3698.
(53) Fujisawa, K.; Ono, T.; Ishikawa, Y.; Amir, N.; Miyashita, Y.; Okamoto, K.; Lehnert, N. *Inorg. Chem.* **2006**, *45*, 1698–1713.
(54) Rondelez, Y.; Séneque, O.; Rager, M.-N.; Duprat, A. F.; Reinaud, O. *Chem.—Eur. J.* **2000**, *6*, 4218–4226.
(55) Kretzer, R. M.; Ghiladi, R. A.; Lebeau, E. L.; Liang, H.-C.; Karlin, K. D. *Inorg. Chem.* **2003**, *42*, 3016–3025.
(56) Fry, H. C.; Lucas, H. R.; Narducci Sarjeant, A. A.; Karlin, K. D.; Meyer, G. J. *Inorg. Chem.* **2008**, *47*, 241–256.

**Scheme 3**

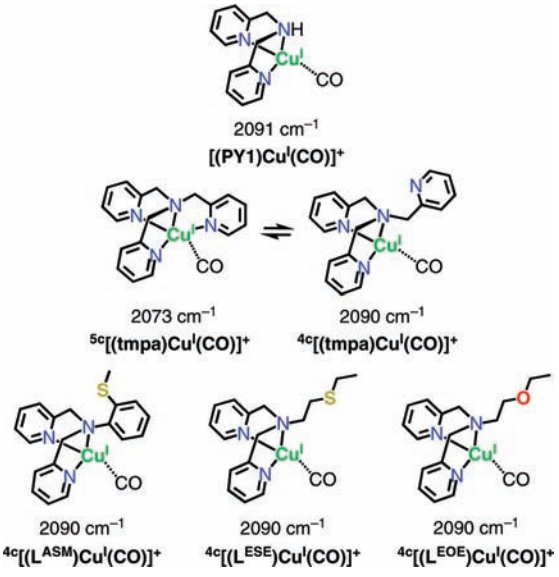


measured by cyclic voltammetry in DMF and $CH_3CN$ solvents under Ar, and compared (side-by-side, under the same conditions, Figure 4) with the behavior of $[(L^{ESE})Cu^{I}]^{+}$ (**2a**) and $[(tmpa)Cu^{I}(CH_3CN)]^{+}$ to assess any differences in tetradentate ligand donor ability. As discussed above, CO-binding experiments did not provide such information because the thioether ligand arm did not coordinate. $E_{1/2}$ values (vs $[Fe(Cp)_2]^{+/0}$) for the compounds are listed in Table 3. All exhibit quasi-reversible one-electron redox processes. There is a marked difference in $E_{1/2}$ values for the three compounds with the TMPA-complex being most negative (favoring Cu(II) relative to Cu(I)), while the $L^{ASM}$ complex has the most positive redox potential. Thus, the two thioether containing ligands raise the complex $E_{1/2}$ values relative to the pyridyl donor in TMPA, presumably because of the well-established and favorable "soft−soft" cuprous ion/thioether interactions.[33,57] Comparing the redox couples of $L^{ASM}$ and $L^{ESE}$, the former is a poorer donor to the copper in $[(L^{ASM})Cu^{I}]^{+}$ (**1a**) versus $[(L^{ESE})Cu^{I}]^{+}$ (**2a**), Table 3, and this finding is consistent to the differences observed crystallographically, in which the Cu−S distance in **1a** is slightly longer than that of **2a** (vide supra). Thus, the ethylthioether group in $L^{ESE}$ is more electron-donating compared to the thioanisole moiety in $L^{ASM}$. It is noteworthy that another important factor for $E_{1/2}$ variations among copper complexes is chelate ring size. In the present case, this factor is not at work given the design of the ligands in which all chelate ring sizes are five-membered. Small differences might be expected because of changes in hybridization as in the thioanisole versus ethylthioether moieties in **1a** and **2a**; however, the structural data shows those angles to be the same.

**X-ray Structure of a Cu(II) Complex with the $N_3S$ Thioether Ligand $L^{ASM}$.** To better understand the nature of copper(II) ion binding with the tripodal ligands being studied here, a copper(II) complex with $L^{ASM}$ was synthesized. X-ray quality crystals could be obtained for $[(L^{ASM})Cu^{II}(CH_3OH)]^{2+}$ (**1c**), Figure 5.

Figure 5 depicts the solid-state structure of $[(L^{ASM})Cu^{II}(CH_3OH)]^{2+}$ (**1c**), revealing that thioether sulfur-$Cu^{II}$ coordination does in fact occur, Cu−S = 2.5276 (6) Å. This suggests that an interaction with this S-donor ligand may also occur in the peroxo complex which forms from the **1a**/$O_2$ reaction, see below. The other three nitrogen atoms in $L^{ASM}$ and one solvent derived methanol O-ligand are bound in equatorial positions; the copper(II) atom sits 0.1033(9) Å out of the best plane formed by N1, N2, N3 and O1 (*rms* deviation = 0.0998 Å) (Figure 5). Hexacoordination is completed by weak ligation from an oxygen atom of a perchlorate anion, Cu−O = 2.6160 (17) Å (Figure 5). This structure is very reminiscent of the closely related and previously reported[25] thioether $L^{ESE}$-copper(II) structure, $[(L^{ESE})Cu^{II}(CH_3OH)]^{2+}$ (**2c**), Figure 6. A comparison of bond distances and angles for **1c** versus **2c** shows most to be nearly identical (Table 4); there is a noticeable elongation of the $Cu^{II}-S_{thioether}$ bond distance (by 0.13 Å) in the $L^{ASM}$ complex **1c**.[59,60]

**Solution Behavior of $[(L^{ASM})Cu^{II}(CH_3OH)]^{2+}$ (1c); EPR Spectroscopy.** A frozen solution EPR spectrum of $[(L^{ASM})Cu^{II}(CH_3OH)]^{2+}$ (**1c**) indicates a typical axial signature (Figure 7) suggesting **1c** is either 6-coordinate like in the X-ray structure (vide supra) or possibly five-coordinate but with SP or distorted SP coordination geometry. The EPR spectrum and derived spectral parameters are very similar to those observed for $[(L^{ESE})Cu^{II}(CH_3OH)]^{2+}$ (**2c**).[25] It is not in a trigonal bipyramidal (TBP) environment, the geometry most often found for five-coordinate complexes with TMPA, $[(tmpa)Cu^{II}\text{-}X]^{2+/+}$ (X = $H_2O$, $CH_3CN$, $Cl^-$).[61−63] The optical spectrum for **1c** (Experimental Section) does not exhibit a distinctive charge-transfer band which might suggest $S_{thioether}$ coordination.[41,42,59,64−72] However, an axial

(57) Ambundo, E. A.; Deydier, M.-V.; Grall, A. J.; Aguera-Vega, N.; Dressel, L. T.; Cooper, T. H.; Heeg, M. J.; Ochrymowycz, L. A.; Rorabacher, D. B. *Inorg. Chem.* **1999**, *38*, 4233–4242.
(58) Fry, H. C. Ph.D. Dissertation, Johns Hopkins University, Baltimore, MD, 2004.
(59) Gilbert, J. G.; Addison, A. W.; Nazarenko, A. Y.; Butcher, R. J. *Inorg. Chim. Acta* **2001**, *324*, 123–130.
(60) Description of the coordination geometry around Cu(II) in each complex, **1c** and **2c**, as if they were pentacoordinate and without the axially weakly bound perchlorate O-donor, indicates that both are distorted from square-based pyramidal, $\tau$ = 0.24 and 0.25, respectively; $\tau$ = 0.0 for a perfect square pyramid (SP); $\tau$ = 1 for a perfect trigonal bipyramidal (TBP) geometry; see: Addison, A. W.; Rao, T. N.; Reedijk, J.; van Rijn, J.; Verschoor, G. C. *J. Chem. Soc., Dalton Trans.* **1984**, 1349–1356.
(61) Karlin, K. D.; Hayes, J. C.; Shi, J.; Hutchinson, J. P.; Zubieta, J. *Inorg. Chem.* **1982**, *21*, 4106–4108.
(62) Zubieta, J.; Karlin, K. D.; Hayes, J. C. Structural Systematics of Cu(I) and Cu(II) Derivatives of Tripodal Ligands. In *Copper Coordination Chemistry: Biochemical and Inorganic Perspectives*; Karlin, K. D., Zubieta, J., Eds.; Adenine Press: Albany, NY, 1983; pp 97−108.
(63) Fox, S.; Nanthakumar, A.; Wikström, M.; Karlin, K. D.; Blackburn, N. J. *J. Am. Chem. Soc.* **1996**, *118*, 24–34.
(64) Lee, Y.; Lee, D. H.; Narducci Sarjeant, A. A.; Zakharov, L. N.; Rheingold, A. L.; Karlin, K. D. *Inorg. Chem.* **2006**, *45*, 10098–10107.
(65) Aronne, L.; Dunn, B. C.; Vyvyan, J. R.; Souvignier, C. W.; Mayer, M. J.; Howard, T. A.; Salhi, C. A.; Goldie, S. N.; Ochrymowycz, L. A.; Rorabacher, D. B. *Inorg. Chem.* **1995**, *34*, 357–369.
(66) Mandal, S.; Bharadwaj, P. K. *Indian J. Chem.* **1991**, *30A*, 948–951.
(67) Bouwman, E.; Driessen, W. L.; Reedijk, J. *Coord. Chem. Rev.* **1990**, *104*, 143–172.
(68) Solomon, E. I.; Penfield, K. W.; Wilcox, D. E. *Struct. Bonding* (*Berlin*) **1983**, *53*, 1–57.
(69) Nikles, D. E.; Powers, M. J.; Urbach, F. L. *Inorg. Chem.* **1983**, *22*, 3210–3217.
(70) Ferris, N. S.; Woodruff, W. H.; Rorabacher, D. B.; Jones, T. E.; Ochrymowycz, L. A. *J. Am. Chem. Soc.* **1978**, *100*, 5939–5942.
(71) Amundsen, A. R.; Whelan, J.; Bosnich, B. *J. Am. Chem. Soc.* **1977**, *99*, 6730–6739.
(72) Miskowski, V. M.; Thich, J. A.; Solomon, R.; Schugar, H. J. *J. Am. Chem. Soc.* **1976**, *98*, 8344–8350.

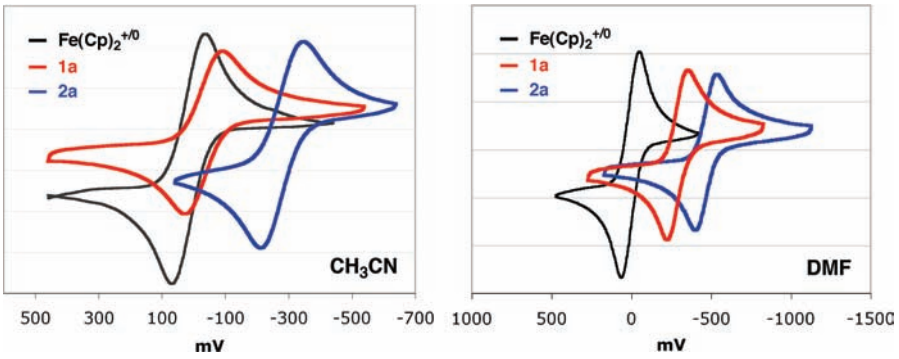


**Figure 4.** Cyclic voltammograms of $[(L^{ASM})Cu^{I}]^{+}$ (**1a**, **red**) and $[(L^{ESE})Cu^{I}]^{+}$ (**2a**, **blue**) measured in $CH_3CN$ (left) and DMF (right) under Ar. $E_{1/2}$ values reported (Table 3) are versus $[Fe(Cp)_2]^{+/0}$ (**black**) measured as an external standard under the same conditions.

**Table 3.** Cyclic Voltammetry Data for Cuprous Complexes in $CH_3CN$ and DMF[a]

| | in $CH_3CN$ | | | in DMF | | |
|---|---|---|---|---|---|---|
| compounds | $E_{pc}$ | $E_{pa}$ | $E_{1/2}$ | $E_{pc}$ | $E_{pa}$ | $E_{1/2}$ |
| $[(tmpa)Cu^{I}(CH_3CN)]^{+}$ | *b* | *b* | −400[25,58] | −640 | −580 | −610 |
| $[(L^{ESE})Cu^{I}]^{+}$ (**2a**) | −350 | −210 | −280 | −410 | −545 | −480 |
| $[(L^{ASM})Cu^{I}]^{+}$ (**1a**) | −110 | +10 | −50 | −230 | −365 | −300 |

[a] mV vs $[Fe(Cp)_2]^{+/0}$. [b] $\Delta E_p \sim 100$ mV.[58]

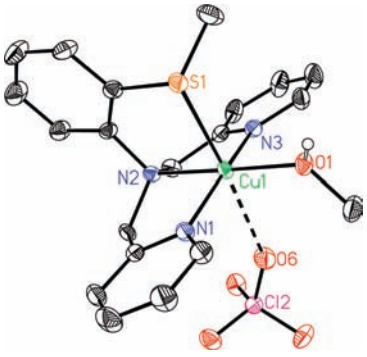


**Figure 5.** Molecular structure of a cationic portion $\{[(L^{ASM})Cu^{II}(CH_3OH)](ClO_4)\}^{+}$ $\{(\mathbf{1c})ClO_4\}$ from X-ray crystallographic analysis. A noncoordinated perchlorate counteranion and hydrogen atoms (except that for the coordinated MeOH group) have been omitted for clarity.

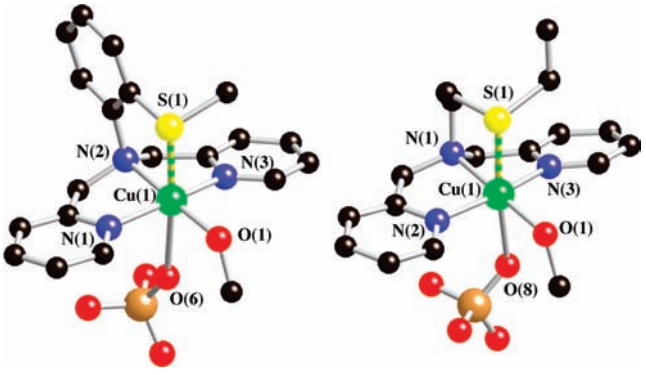


**Figure 6.** Molecular structure comparison between isolated cations of $\{[(L^{ASM})Cu^{II}(CH_3OH)](ClO_4)\}^{+}$ ($[\mathbf{1c}]ClO_4$) and $\{[(L^{ESE})Cu^{II}(CH_3OH)](ClO_4)\}^{+}$ ($[\mathbf{2c}]ClO_4$) derived from X-ray crystallographic analysis. Hydrogen atoms are omitted for clarity.

thioether charge-transfer would not be expected to have much intensity.

**Reductive Dechlorination Reaction of $[(L^{EOE})Cu^{I}]^{+}$ (3a).** Dissolving $[(L^{EOE})Cu^{I}]^{+}$ **3a** in dichloromethane solvent instantly gives a blue solution at room temperature under a nitrogen atmosphere. During a 30 min reaction time, a blue precipitate formed, and the resulting product was isolated in good yield (>90%). ESI mass spectrometry and elemental analysis reveal the product identity as the $LCu^{II}-Cl$ complex shown in the diagram below. The product is derived from a dehalogenation reaction well-known for copper chemistry with TMPA[5,73] and its analogues.[74−78]

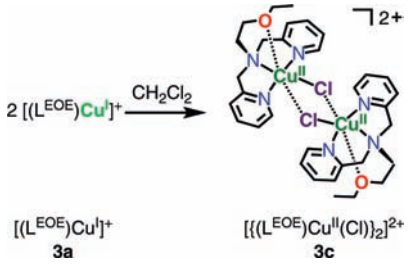


A suitable single crystal was obtained for $[\{(L^{EOE})Cu^{II}(Cl)\}_2]^{2+}$ (**3c**). The geometry of the cupric ion is distorted octahedral with three nitrogen donors and one chloride anion in equatorial positions (Figure 8). The ether oxygen donor is weakly axially coordinated to the copper ion, $Cu\cdots O$ = 2.4765 Å), while the other chloride ligand from the partner complex is weakly occupied in the other axial position with much longer distance (2.9536 Å). Pentacoordination in mononuclear complexes is more typical for such tripodal tetradentate ligands with all N donors, for example, $(ligand)Cu^{II}-Cl$,[5,74−78] It seems that with the weak $O_{ether}$ donor, the cupric ion is able to also interact with a sixth ligand, here the chloride from the other ligand-copper(II) moiety, to form the observed dimer.

(73) Jacobson, R. R.; Tyeklár, Z.; Karlin, K. D. *Inorg. Chim. Acta* **1991**, *181*, 111–118.
(74) Lucchese, B.; Humphreys, K. J.; Lee, D.-H.; Incarvito, C. D.; Sommer, R. D.; Rheingold, A. L.; Karlin, K. D. *Inorg. Chem.* **2004**, *43*, 5987–5998.
(75) Lee, D.-H.; Wei, N.; Murthy, N. N.; Tyeklár, Z.; Karlin, K. D.; Kaderli, S.; Jung, B.; Zuberbühler, A. D. *J. Am. Chem. Soc.* **1995**, *117*, 12498–12513.
(76) Wei, N.; Murthy, N. N.; Chen, Q.; Zubieta, J.; Karlin, K. D. *Inorg. Chem.* **1994**, *33*, 1953–1965.
(77) Wei, N.; Murthy, N. N.; Karlin, K. D. *Inorg. Chem.* **1994**, *33*, 6093–6100.
(78) Wei, N.; Murthy, N. N.; Tyeklár, Z.; Karlin, K. D. *Inorg. Chem.* **1994**, *33*, 1177–1183.

**Table 4.** Selected Bond Distances and Angles of $[(L^{ASM})Cu^{II}(CH_3OH)]^{2+}$ (**1c**) and $[(L^{ESE})Cu^{II}(CH_3OH)]^{2+}$ (**2c**)[25]

| $[(L^{ASM})Cu^{II}(CH_3OH)]^{2+}$ (**1c**) | | $[(L^{ESE})Cu^{II}(CH_3OH)]^{2+}$ (**2c**)[25] | |
|---|---|---|---|
| Cu−X | bond distance (Å) | Cu−X | bond distance (Å) |
| Cu(1)−N(1) | 1.9746 (17) | Cu(1)−N(2) | 1.981 (2) |
| Cu(1)−N(2) | 2.0573 (16) | Cu(1)−N(1) | 2.0302 (19) |
| Cu(1)−N(3) | 1.9712 (17) | Cu(1)−N(3) | 1.983 (2) |
| Cu(1)−S(1) | 2.5276 (6) | Cu(1)−S(1) | 2.6551 (7) |
| Cu(1)−O(1) | 2.0029 (14) | Cu(1)−O(1) | 2.0009 (17) |
| Cu(1)−O(6)[a] | 2.6160 (17) | Cu(1)−O(8)[a] | 2.57 (1) |
| $[(L^{ASM})Cu^{II}(CH_3OH)]^{2+}$ (**1c**) | | $[(L^{ESE})Cu^{II}(CH_3OH)]^{2+}$ (**2c**)[25] | |
| X−Cu−X | bond angle (deg) | X−Cu−X | bond angle (deg) |
| N(1)−Cu(1)−N(3) | 163.36 (7) | N(2)−Cu(1)−N(3) | 164.01 (8) |
| N(1)−Cu(1)−N(2) | 84.28 (7) | N(1)−Cu(1)−N(2) | 84.41 (8) |
| N(2)−Cu(1)−N(3) | 84.07 (7) | N(3)−Cu(1)−N(1) | 82.20 (8) |
| N(1)−Cu(1)−O(1) | 97.79 (6) | N(1)−Cu(1)−O(1) | 178.94 (8) |
| N(2)−Cu(1)−O(1) | 177.89 (6) | N(2)−Cu(1)−O(1) | 96.36 (8) |
| N(3)−Cu(1)−O(1) | 93.82 (7) | N(3)−Cu(1)−O(1) | 96.93 (8) |
| N(1)−Cu(1)−S(1) | 91.80 (5) | N(1)−Cu(1)−S(1) | 87.61 (6) |
| N(2)−Cu(1)−S(1) | 87.79 (5) | N(2)−Cu(1)−S(1) | 90.00 (6) |
| N(3)−Cu(1)−S(1) | 99.57 (5) | N(3)−Cu(1)−S(1) | 98.11 (6) |
| O(1)−Cu(1)−S(1) | 92.57 (5) | O(1)−Cu(1)−S(1) | 93.13 (6) |

[a] One perchlorate anion coordinates very weakly to Cu(1).

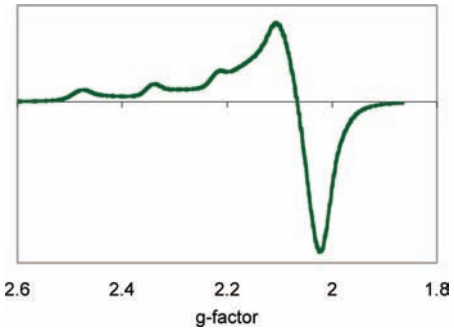


**Figure 7.** EPR spectra of $[(L^{ASM})Cu^{II}(CH_3OH)]^{2+}$ (**1c**) taken with an X-band spectrometer ($\nu$ = 9.186 GHz) in 2-methyltetrahydrofuran (MeTHF)/$CH_3CN$ (1:1) at 77 K. $g_{\|}$ = 2.28, $A_{\|}$ = 158 gauss; $g_{\perp}$ = 2.06.

Selected bond distances and angles for **3c** are listed in Table 5.

**Dioxygen Reactivity of $[(L^{ASM})Cu^{I}]^{+}$ (1a·B(C$_6$F$_5$)$_4$); End-on Peroxo-Dicopper(II) Formation.** Dioxygen reacts reversibly with 2 equiv of $[(L^{ASM})Cu^{I}]^{+}$ (**1a**) in 2-methyltetrahydrofuran (MeTHF) at −125 °C, forming the low-temperature stable deep blue species $[\{(L^{ASM})Cu^{II}\}_2(O_2^{2-})]^{2+}$ (**1b$^{P}$**). This exhibits UV−visible absorptions at 442 (1,500 $M^{-1}$ $cm^{-1}$), 530 (8,600 $M^{-1}$ $cm^{-1}$), and 605 nm (10,400 $M^{-1}$ $cm^{-1}$) (Table 6), (spectrum **B**, Figure 9). The prominent LMCT transitions occur in the region (500 to 650 nm), an energy region typical for end-on peroxo species;[2] however, the ∼600 nm absorption region is relatively more intense. This appears to be a consequence of the thioether ligation; we observed this same absorption pattern with a peroxo species derived from the analogue thioether ligand chelate $L^{ESE}$ (Chart 2).[24,25] There, analysis of the spectroscopic data (including resonance Raman spectroscopy) showed that the strong low-energy UV−vis feature in $[\{(L^{ESE})Cu^{II}\}_2(O_2^{2-})]^{2+}$ (**2b$^{P}$**) was not from a Cu−S charge transfer band, but rather the result of a geometric change around the cupric center of the peroxo complex. The coordination geometry is distorted toward square-based pyramidal (SP) compared to the TBP geometry (with axial peroxo O-ligand) known for $[\{(tmpa)Cu^{II}\}_2(O_2^{2-})]^{2+}$ (Scheme 1). EXAFS data clearly revealed that the thioether sulfur atom of $L^{ESE}$ coordinates to copper in $[\{(L^{ESE})Cu^{II}\}_2(O_2^{2-})]^{2+}$, with a Cu−S vector of 2.4 Å.[24] We do not have corresponding data for $[\{(L^{ASM})Cu^{II}\}_2(O_2^{2-})]^{2+}$ (**1b$^{P}$**); however, given the close similarity of $L^{ASM}$ and $L^{ESE}$ $N_3S_{thioether}$ ligands (Chart 1),

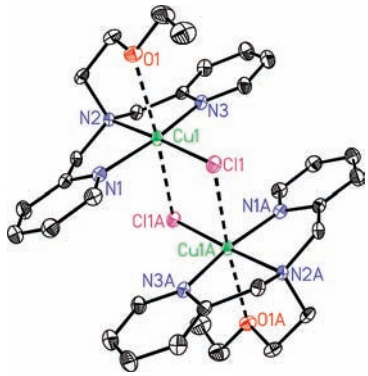


**Figure 8.** X-ray structure of a cationic portion $[\{(L^{EOE})Cu^{II}(Cl)\}_2]^{2+}$ (**3c**). The $B(C_6F_5)_4^-$ counteranion and hydrogen atoms are omitted from the ORTEP view for clarity.

**Table 5.** Selected Bond Distances and Angles of $[\{(L^{EOE})Cu^{II}(Cl)\}_2]^{2+}$ (**3c**)

| Cu−X | bond distance (Å) | X−Cu−X | bond angle (deg) |
|---|---|---|---|
| | | N(1)−Cu(1)−N(3) | 165.40 (8) |
| Cu(1)−N(1) | 1.979 (2) | N(1)−Cu(1)−N(2) | 82.13 (8) |
| Cu(1)−N(2) | 2.0418 (19) | N(2)−Cu(1)−N(3) | 83.62 (8) |
| Cu(1)−N(3) | 1.9854 (19) | N(1)−Cu(1)−Cl(1) | 96.33 (6) |
| Cu(1)−O(1) | 2.4765 (16) | N(3)−Cu(1)−Cl(1) | 97.77 (6) |
| Cu(1)−Cl(1) | 2.2305 (6) | N(2)−Cu(1)−Cl(1) | 177.25 (5) |
| Cu(1)−Cl(1A) | 2.9536 (6) | N(1)−Cu(1)−O(1) | 97.15 (7) |
| Cu(1)−Cu(1A) | 3.6254 (5) | N(3)−Cu(1)−O(1) | 83.23 (7) |
| | | N(2)−Cu(1)−O(1) | 79.10 (6) |
| | | Cl(1)−Cu(1)−O(1) | 103.38 (4) |

**Table 6.** UV-vis and Resonance Raman Spectroscopic Data for Tripodal Ligand Copper-Dioxygen Adducts

| complex | LMCT; $\lambda_{max}$ nm ($\varepsilon$ $M^{-1}$ $cm^{-1}$) | | | solvent temp | $\nu$(O−O); $\Delta(^{18}O_2)$; $cm^{-1}$ | $\nu_{sym}$(Cu−O); $\Delta(^{18}O_2)$ $cm^{-1}$ |
|---|---|---|---|---|---|---|
| $[\{(tmpa)Cu^{II}\}_2(O_2^{2-})]^{2+}$[79] | 435 (1,700) | 524 (11,300) | 615 (5,800) | EtCN −80 °C | 832; −44 | 561; −26 [a] |
| $[\{(tmpa)Cu^{II}\}_2(O_2^{2-})]^{2+}$[80] | 430 (2,100) | 520 (12,000) | 590 (8,000) | MeTHF −128 °C | | |
| $[\{(L^{ESE})Cu^{II}\}_2(O_2^{2-})]^{2+}$ (**2b$^{P}$**)[24] | 445 (2,600) | 530 (9,200) | 605 (11,800) | MeTHF −128 °C | 817; −46 | 545; −26 [b] |
| $[\{(L^{ASM})Cu^{II}\}_2(O_2^{2-})]^{2+}$ (**1b$^{P}$**) | 442 (1,500) | 530 (8,600) | 605 (10,400) | MeTHF −128 °C | 828; −48 | 547; −23 |

[a] The values were obtained with $[\{(tmpa)Cu^{II}\}_2(O_2^{2-})]^{2+}$ as a powder; in propionitrile solution at 190 K, the 832 and 561 $cm^{-1}$ peaks shift to 826 and 554 $cm^{-1}$, respectively. [b] Resonance Raman measurements were carried out in $CH_2Cl_2$ as solvent.

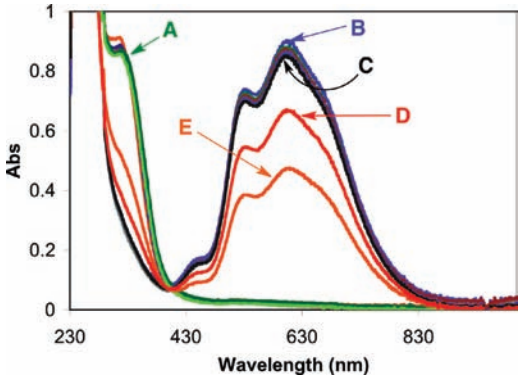


**Figure 9.** Low-temperature UV−vis spectra: **A** (**green**): **1a** with absorption at 318 nm, $\varepsilon$ 5,100 $M^{-1}$ $cm^{-1}$. **B** (**blue**): **1b$^{P}$** with absorption at 445 ($\varepsilon$ 1,500 $M^{-1}$ $cm^{-1}$), 530 ($\varepsilon$ 8,600 $M^{-1}$ $cm^{-1}$), and 605 nm ($\varepsilon$ 10,400 $M^{-1}$ $cm^{-1}$) in MeTHF at −125 °C. **A**, **B**, and **C** (multiple spectra in a different colors): five cycles by vacuum/purging of **1b$^{P}$** and $O_2$ bubbling of **1a**. **D** (**red**): At −100 °C, warmed from −125 °C, the absorption intensity due to **3b$^{P}$** is reduced. **E** (**orange**): At −94 °C, warmed from −125 °C, the absorption intensity due to **3b$^{P}$** is further reduced. See text.

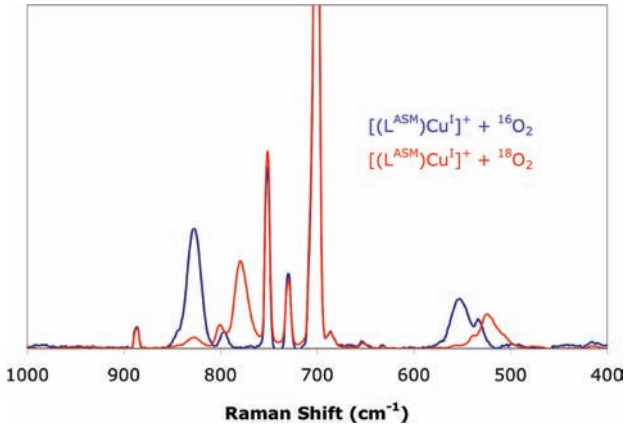


**Figure 10.** Resonance Raman spectra of $[\{(L^{ASM})Cu^{II}\}_2(O_2^{2-})]^{2+}$ (**1b$^{P}$**) in THF at 77 K (blue spectrum denotes $^{16}O_2$, red spectrum denotes $^{18}O_2$. $\lambda_{ex}$ = 568 nm. $\nu$(O−O) = 828 $cm^{-1}$($\Delta(^{18}O_2)$ = 48), $\nu_{sym}$(Cu−O) = 547 $cm^{-1}$ ($\Delta(^{18}O_2)$ = 23) and $\nu_{asym}$(Cu−O) = 497 $cm^{-1}$ ($\Delta(^{18}O_2)$ = 22).

along with the very closely matching UV−visible absorption envelope (and see further discussion and Figure below), we conclude that **1b$^{P}$** possesses the same structure as **2b$^{P}$** and includes thioether S-ligation.

After applying a vacuum and purging with Ar at −125 °C in MeTHF led to the removal of $O_2$ from $[\{(L^{ASM})Cu^{II}\}_2(O_2^{2-})]^{2+}$ (**1b$^{P}$**), and yellow solutions of **1a** (spectrum **A**, Figure 9) can be regenerated. A second low-temperature oxygenation allowed full reformation of **1b$^{P}$**, which indicates that little or no irreversible decomposition occurs at reduced temperatures (below −80 °C). In fact, five oxygenation-deoxygenation cycles could be carried out, with the final spectrum (**C**, Figure 9) being essentially identical to the first. We find that the peroxo **1b$^{P}$** and cuprous complex (**1a**) equilibrium is sensitive to the solution temperature. An increase of ∼30 degrees in temperature resulted in a ∼40% decrease in absorption of **1b$^{P}$**, spectrum **E** (Figure 9) measured at −94 °C. We note that the oxygenation and UV−vis behavior of **1a** and **2a** are the same as that observed for warmer solutions (∼−90 °C) in THF and $CH_2Cl_2$ solvents.

**Resonance Raman Spectroscopic Characterization of $[\{(L^{ASM})Cu^{II}\}_2(O_2^{2-})]^{2+}$ (1b$^{P}$).** Resonance Raman spectra also support the formation and formulation of the peroxo-dicopper(II) species $[\{(L^{ASM})Cu^{II}\}_2(O_2^{2-})]^{2+}$ (**1b$^{P}$**) (Figure 10). Isotope dependent features were observed both at 828 $cm^{-1}$ ($\Delta(^{18}O_2)$ = 48) and 547 $cm^{-1}$ ($\Delta(^{18}O_2)$ = 23). On the basis of their energies and reduced mass considerations following $^{18}O_2$ isotope substitution, the features are assigned as the $\nu$(O−O) and $\nu$(Cu−O) modes, respectively. These occur in the range of those previously found for a *trans*-$\mu$-1,2-peroxodicopper(II) complex.[2,24,25,79] Table 6 summarizes resonance Raman spectroscopic data for **1b$^{P}$**, the closely related **2b$^{P}$**, and the TMPA complex with all nitrogen donor ligands, $[\{(tmpa)Cu^{II}\}_2(O_2^{2-})]^{2+}$. Both the $\nu$(O−O) and $\nu$(Cu−O) stretching vibrations occur at lower energy than is found in $[\{(tmpa)Cu^{II}\}_2(O_2^{2-})]^{2+}$, (832 and 561 $cm^{-1}$, respectively). As reported $[\{(L^{ESE})Cu^{II}\}_2(O_2^{2-})]^{2+}$ (**2b$^{P}$**) similarly shows weakening of the O−O and Cu−O bonds compared to $[\{(tmpa)Cu^{II}\}_2(O_2^{2-})]^{2+}$.[24,25] As already explained in detail for the case of **2b$^{P}$**, these changes occur from a combination of factors; the thioether ligand acts as a good (electronic) donor, and geometric distortions from TBP occur, probably because of the ligand structure changes put in place by $L^{ESE}$ and $L^{ASM}$ compared to TMPA. As discussed above from cuprous structures for **1a** and **2a** and their electrochemistry, the thioanisole moiety seems to behave as a poorer donor ligand than the alkyl thioether. It is interesting that both the $\nu$(O−O) and the $\nu$(Cu−O) for **1b$^{P}$** are higher than that for **2b$^{P}$** which is consistent with the structural and electrochemistry results for their cuprous complexes, that is, that the thioanisole S-atom in $L^{ASM}$ is a poorer donor that is the alkyl-thioether S-donor in $L^{ESE}$.

**Dioxygen Complex Reactivity with $[(L^{EOE})Cu^{I}]^{+}$ (3a).** To further provide (indirect) chemical evidence that sulfur coordination is also involved in peroxo complexes $[\{(L^{ASM})Cu^{II}\}_2(O_2^{2-})]^{2+}$ (**1b$^{P}$**) and $[\{(L^{ESE})Cu^{II}\}_2(O_2^{2-})]^{2+}$ (**2b$^{P}$**), we examined the copper(I)/$O_2$ reactivity with the ether analogue, $L^{EOE}$ (Chart 1). Oxygenation of $[(L^{EOE})Cu^{I}]^{+}$ (**3a**) leads to formation of a new species with prominent optical absorption at 380 nm ($\varepsilon \sim 10{,}000$ $M^{-1}$ $cm^{-1}$, **b** in Figure 11). On the basis of established UV−vis criteria,[2] a bis($\mu$-oxo) complex $[\{(L^{EOE})Cu^{III}\}_2(O^{2-})_2]^{2+}$ (**3b$^{O}$**) formed, and not an end-on peroxo species. Copper(I) complexes with tridentate

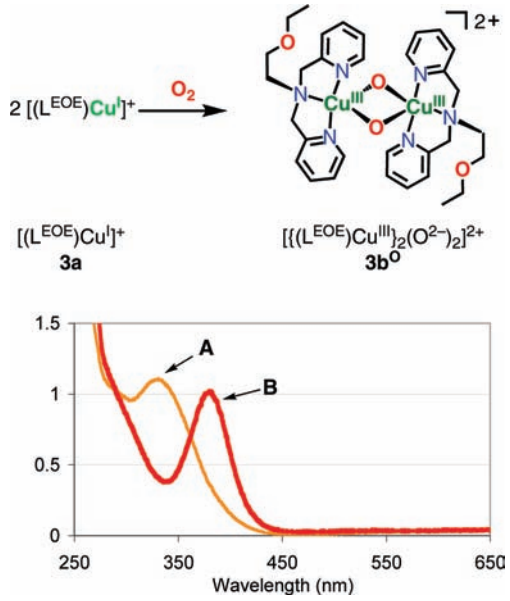


**Figure 11.** Low-temperature UV−vis spectra of **A**: $[(L^{EOE})Cu^{I}]^{+}$ (**3a**) absorption at 329 nm, 5,000 $M^{-1}$ $cm^{-1}$, **B**: $[\{(L^{EOE})Cu^{III}\}_2(O^{2-})_2]^{2+}$ (**3b$^{O}$**) absorption 380 nm (10,000 $M^{-1}$ $cm^{-1}$) in THF at −94 °C.

**Scheme 4**

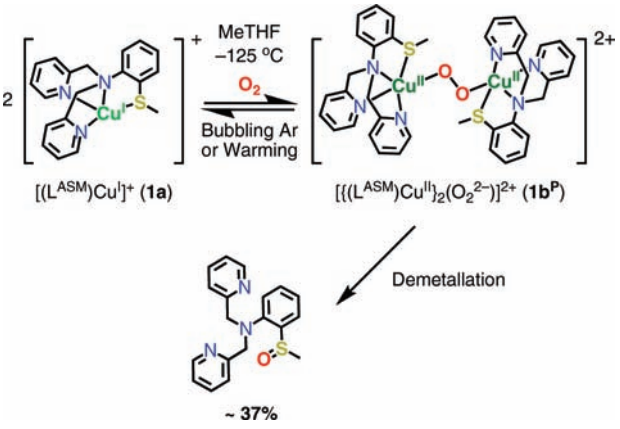


ligands like the PY1 moiety in $L^{EOE}$ give bis($\mu$-oxo) dicopper(III) complexes;[47,81,82] the fact that this does not occur with $L^{ASM}$ and $L^{ESE}$, supports the idea that the sulfur atom is coordinated in **1b$^{P}$** and **2b$^{P}$**.

**Sulfoxidation of $L^{ASM}$ in 1b$^{P}$.** A green solution was obtained following warming solutions of $[\{(L^{ASM})Cu^{II}\}_2(O_2^{2-})]^{2+}$ (**1b$^{P}$**) to RT. After a demetallation procedure, the decomposition product was isolated and identified as the sulfoxide derivative of $L^{ASM}$, obtained in moderate yield (~ 37%), Scheme 4 (see Experimental Section). The same behavior was also observed for **2b$^{P}$**, and the corresponding sulfoxide product of $L^{ESE}$ was obtained in 44% yield.[25] This kind of behavior suggests a monooxygenase

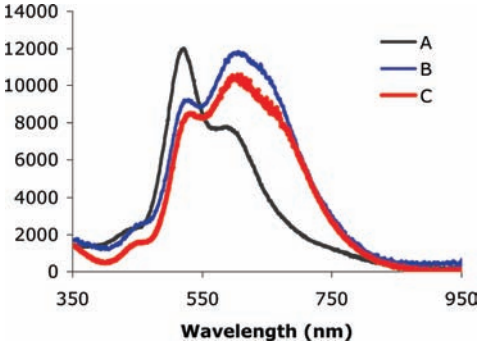


**Figure 12.** Low-temperature UV−vis spectra: **A** (black), $[\{(tmpa)Cu^{II}\}_2(O_2^{2-})]^{2+}$; **B** (blue), $[\{(L^{ESE})Cu^{II}\}_2(O_2^{2-})]^{2+}$ (**2b$^{P}$**); and **C** (red), $[\{(L^{ASM})Cu^{II}\}_2(O_2^{2-})]^{2+}$ (**1b$^{P}$**).

type reaction and stoichiometry.[64] An $^{18}O_2$ labeling experiment revealed dioxygen as the source of the sulfoxide oxygen atom. Thus, ESI and FAB mass spectrometry obtained on both the $(L^{AS(O)M})$-copper(II) complex in the reaction product mixture, as well as with the isolated sulfoxide organic (following demetallation), indicate that the oxygen atom is transferred to $L^{ASM}$ from labeled $^{18}O_2$ in **1b$^{P}$** with >90% incorporation (See Experimental Section). It is interesting to note that Kodera and coworkers[41] did not observe any thioether oxidation when generating a copper(II)-OOH species using a ligand with an −SPh moiety.

**Comparisons of $[\{(L^{ASM})Cu^{II}\}_2(O_2^{2-})]^{2+}$ (1b$^{P}$) versus $[\{(L^{ESE})Cu^{II}\}_2(O_2^{2-})]^{2+}$ (2b$^{P}$).** As stated, the electronic absorption spectra of both $[\{(L^{ASM})Cu^{II}\}_2(O_2^{2-})]^{2+}$ (**1b$^{P}$**) and $[\{(L^{ESE})Cu^{II}\}_2(O_2^{2-})]^{2+}$ (**2b$^{P}$**) show an inversion in intensity of the two dominant LMCT bands (~ 500 and ~600 nm) compared with those observed in $[\{(tmpa)Cu^{II}\}_2(O_2^{2-})]^{2+}$, Figure 12.[24,25] For **2b$^{P}$**, it was previously determined to reflect the presence of the $S_{thioether}$ donor and a peroxide ligand $\pi^*_\sigma/\pi^*_\nu$ inversion, likely a result of a copper(II) geometry distorted toward SP.[24,25] As **2b$^{P}$** possesses an extremely similar LMCT pattern (and of course the $L^{ASM}$ and $L^{ESE}$ ligands are similar), the same analysis would apply to **1b$^{P}$**. As described, structural comparisons of $[(L^{ASM})Cu^{II}(CH_3OH)]^{2+}$ (**1c**) with $[(L^{ESE})Cu^{II}(CH_3OH)]^{2+}$ (**2c**) reveal these to have very similar cupric ion coordination geometries. All of this indirectly supports the similarity observed in the optical spectra of the peroxodicopper(II) complexes derived from these ligands. The electrochemical and structural data accompanied with the resonance Raman analysis suggests that the thioanisole group in **1b$^{P}$** has a poorer electron donating ability compared with the thioether moiety.

## Summary and Conclusions

To provide further insights into the nature of sulfur ligation to copper ion and the resulting oxidative chemistry, we have here described the copper-$O_2$ chemistry with thioanisole containing $N_3S$ ligand $L^{ASM}$, the close analogue of previously reported alkyl thioether ligand $L^{ESE}$.[24,25] The thioanisole moiety in $[(L^{ASM})Cu^{I}]^{+}$ (**1a**) is a poorer donor compared to $[(L^{ESE})Cu^{I}]^{+}$ (**2a**), based on comparative electrochemistry studies, and the observation of a relatively longer Cu−S bond distance in crystal structures of **1a** versus **2a**. Both thioether containing complexes exhibit significant differences in the optical transitions and resonance Raman

(79) Baldwin, M. J.; Ross, P. K.; Pate, J. E.; Tyeklár, Z.; Karlin, K. D.; Solomon, E. I. *J. Am. Chem. Soc.* **1991**, *113*, 8671–8679.
(80) unpublished results.
(81) Kunishita, A.; Osako, T.; Tachi, Y.; Teraoka, J.; Itoh, S. *Bull. Chem. Soc. Jpn.* **2006**, *79*, 1729–1741.
(82) Lucas, H. R.; Li, L.; Sarjeant, A. A. N.; Vance, M. A.; Solomon, E. I.; Karlin, K. D. *J. Am. Chem. Soc.* **2009**, *131*, 3230–3245.

characteristics of their cupric-peroxo binuclear complexes (i.e., their dioxygen adducts) in comparison to the properties observed for the all nitrogen parent compound $[\{(tmpa)Cu^{II}\}_2(O_2^{2-})]^{2+}$. The variations are ascribed to the thioether ligation present in $[\{(L^{ASM})Cu^{II}\}_2(O_2^{2-})]^{2+}$ (**1b$^{P}$**) and $[\{(L^{ESE})Cu^{II}\}_2(O_2^{2-})]^{2+}$ (**2b$^{P}$**) which leads to copper(II) ion local geometric distortions away from TBP toward SP. Support for this postulate includes structural characteristics (SP geometries) observed in X-ray structures of the mononuclear copper(II) analogues, $[(L^{ASM})Cu^{II}(CH_3OH)(ClO_4)]^{+}$ (**1c**) and $[(L^{ESE})Cu^{II}(CH_3OH)(ClO_4)]^{+}$ (**2c**). The poorer thioether ligand donating ability in $L^{ASM}$ compared to $L^{ESE}$ is also manifested in observed resonance Raman spectroscopic variation in **1b$^{P}$** versus **2b$^{P}$**; as seen before, stronger ancillary ligand donation reduces the donor interaction of the peroxide with the Cu orbital that leads to lowering of $\nu$(O−O) and $\nu$(Cu−O);[83] thus both the O−O and Cu−O bonds are weakened relative to $[\{(tmpa)Cu^{II}\}_2(O_2^{2-})]^{2+}$.

(83) Henson, M. J.; Vance, M. A.; Zhang, C. X.; Liang, H.-C.; Karlin, K. D.; Solomon, E. I. *J. Am. Chem. Soc.* **2003**, *125*, 5186–5192.

The correlation of variations (i.e., denticity, donor atom type, chelate ring size) in the nature of coordinating ligands with copper-dioxygen adduct structure and spectroscopy continues to be an area of active inquiry. To this end, we plan to design and investigate new systems, for example, to explore thioether coordination effects on $Cu^{I}/O_2$ chemistry with only two nitrogen donors per copper ion present. Given the observed weakening of O−O an Cu−O bonds in these thioether containing peroxo-dicopper(II) complexes, here and in our other studies,[24,25,45] comparative substrate oxidative reactivity studies are also warranted.

**Acknowledgment.** K.D.K., E.I.S., and M.K.E. are grateful to the NIH for support (GM 28962, DK 031450, GM 085914 (postdoctoral fellowship) respectively). D.H.L. is grateful to Chonbuk National University for support.

**Supporting Information Available:** Crystallographic information files (CIF) for $[(L^{ASM})Cu^{I}]^{+}$ (**1a**), $[(L^{ASM})Cu^{II}(CH_3OH)]^{2+}$ (**1c**), and $[\{(L^{EOE})Cu^{II}(Cl)\}_2]^{2+}$ (**3c**). This material is available free of charge via the Internet at http://pubs.acs.org.